MASTER IN BIOLOGY

Characterization of the replication and segregation of Brucella abortus chromosomes during in vitro culture

Sternon, Jean-François

Award date:
2013

Awarding institution:
University of Namur

FACULTES UNIVERSITAIRES NOTRE-DAME DE LA PAIX
NAMUR

Faculté des Sciences

Characterization of the replication and segregation of *Brucella abortus* chromosomes during *in vitro* culture

Mémoire présenté pour l'obtention

du grade académique de master en biochimie et biologie moléculaire et cellulaire

Jean-François STERNON

Janvier 2013

Facultés Universitaires Notre-Dame de la Paix
FACULTE DES SCIENCES
Secrétariat du Département de Biologie
Rue de Bruxelles 61 - 5000 NAMUR
Téléphone: + 32(0)81.72.44.18 - Téléfax: + 32(0)81.72.44.20
E-mail: joelle.jonet@fundp.ac.be - http://www.fundp.ac.be/fundp.html

Caractérisation de la réplication et de la ségrégation des chromosomes de *Brucella abortus* en culture *in vitro*

STERNON Jean-François

Résumé

Les bactéries du genre *Brucella* sont les agents pathogènes responsables de la brucellose, une maladie de type « anthropo-zoonose » connue pour être la plus répandue au monde. Il a été récemment mis en évidence que lors du cycle infectieux de *Brucella abortus*, caractérisé par une phase non-prolifération dans les premières heures de l'infection de cellules eucaryotes hôtes, la majorité des bactéries observées affichent un phénotype PdhS-/IfoP+, habituellement observé de manière transitoire en culture, et conséquente à la division asymétrique de *Brucella*. En conséquence, cette observation suggère l'hypothèse d'un blocage du cycle cellulaire du pathogène à une phase particulière durant les premières heures de son cycle infectieux.

Dans le but de tester cette hypothèse, nous avons créé différentes souches de *B. abortus* permettant de localiser des régions chromosomiques correspondant aux origines et aux terminateurs des deux chromosomes (I et II) de la bactérie. Les observations qui en découlent ont pour but de mettre en évidence l'initiation et/ou la terminaison de la réplication de ses deux chromosomes. À l'aide de ces systèmes rapporteurs, nous avons pu déterminer que l'origine (*ori*) et le terminateur (*ter*) de chaque chromosome (*ori*I/*ori*II et *ter*I/*ter*II) présentent des patterns de localisation spécifiques et reproductibles au sein de la cellule.

Les origines adoptent une localisation focalisée au niveau du vieux pole bactérien dans les bactéries de petite taille. Pour les bactéries de plus grande taille et en cours de division, un second focus dupliqué est observé pour chaque origine, adoptant en majorité une localisation bipolaire de nature identique à celle décrite ci-dessus. Les terminateurs quant à eux adoptent une localisation récurrente au niveau du nouveau pole bactérien dans les cellules de petite taille. Dans les cellules de plus grande taille et en cours de division, ces régions se trouvent au niveau de l'emplacement du site de constriction. Il est a noté que, si pour *ter*II la présence de deux foci dans les grandes cellules est facilement observable, aucune bactérie observée ne montre la présence de deux foci pour *ter*I, même dans les cellules en fin de constriction. De manière intéressante, la localisation des régions précitées n'est pas identique pour les deux chromosomes, ce qui est en accord avec l'hypothèse d'une origine évolutive divergente pour ces deux éléments.

Finalement, l'étude de la localisation des deux chromosomes de *Brucella abortus* est cohérente avec des données antérieures portant sur la localisation des machineries de ségrégation de ces chromosomes. La localisation de ces systèmes de ségrégation pourrait donc permettre l'identification de l'état de réplication du pathogène *Brucella abortus* au cours d'une infection cellulaire, et donc une meilleure caractérisation du cycle cellulaire bactérien.

Mémoire de master en biochimie et biologie moléculaire et cellulaire

Janvier 2013

Promoteur: Prof. X. De Bolle

Remerciements

Je tiens tout d'abord à remercier mon promoteur, le professeur Xavier De Bolle, pour les nombreux conseils donnés au cours de ces dix mois, ainsi que pour la passion avec laquelle il arrive à transmettre ses connaissances. Je tiens également à remercier les professeurs Jean-Jacques Letesson et Jean-Yves Matroule pour m'avoir permis de réaliser mon mémoire au sein de ce laboratoire. Ce fut un réel plaisir.

Je tiens également à remercier tout spécialement mon tuteur/encadrant, ex futur docteur Michael Deghelt. Mis appart ces longs moments durant lesquels tu m'expliquais ce dont une femme a besoin pour être « comblée » (en tous cas selon ta conception de l'amour), ou les moments où tu me traitais de sale con sous doué qui n'aurait jamais droit qu'à un sobre remerciement dans ton futur papier dans Cell, ce fut sincèrement un réel plaisir de travailler à tes côtés, tant du point de vue des manips que du point de vue de l'ambiance en général. Un grand merci également aux autres membres de la Xa team, Caro et Nayla, (ainsi qu'à monsieur l'assistant Jérôme Coppine (AAAaaames)) pour avoir supporté mes nombreuses questions et m'avoir coatché durant les 4 mois d'absence de mon tuteur. Votre aide et vos conseils me furent également d'une grande aide pour mener à bien mes manips.

Ensuite, de manière plus générale, je souhaiterais remercier tout les membres de l'URBM pour l'ambiance chaleureuse qui a caractérisé ce mémoire. Je pense tout spécialement à Mr. Lionel Schille, avec qui nous avons toujours de nombreuses vidéos de fails à rattraper ainsi qu'un verger à construire !

Concernant mes camarades mémos de l'URBM (Gautier, Seb (« Bruce »), et Hubert (aux surnoms innombrables et par conséquent non résumables ici), je tiens également à dire merci pour la bonne ambiance qui a régné entre nous 4 durant ces dix mois, et ce malgré les nombreux échecs par lesquels nous sommes tous passés ! Hé oui, nous l'aurons bien compris, la beauté de la théorie est ce qui nous attire dans le labo, là où, par la suite, on se prend une grande claque de la part de la pratique, nous enseignant à la dure que la science, ça ne marche pas (ou en tous cas pas du premier coup, sauf chance de cocu) ! Petite remarque additionnelle pour Hubert : S'il te plait, par pitié, essaye d'arrêter avec tes blagues douteuses… Ou essaye au moins d'en diminuer le débit. Je te promets que pour moi qui ai passé tout mon mémoire en face de toi, la blague de « hé mec…12 !!! » un jeudi à 19 h, ça peut vraiment pousser des gens en condition mentale fragile (aka : nous, autres mémos, qui ne disposons pas de la même fibre humoristique, après une dure journée de travail) à commettre des actes légalement répréhensibles envers ta personne. Ceci étant dis, tu en as quand même lâché des bonnes (ainsi que quelques vraiment, vraiment pas bonnes, mais c'est une autre histoire).

Voila, j'ai très certainement oublié de nombreuses personnes importantes et je m'en excuse d'avance. Encore une fois un grand merci à tous, et à la revoyure !

Chers membres du jury, je vous souhaite une bonne lecture !

« *La théorie, c'est quand on sait tout et que rien ne fonctionne.*

La pratique, c'est quand tout fonctionne et que personne ne sait pourquoi.

Ici, nous avons réuni théorie et pratique : Rien ne fonctionne…

et personne ne sait pourquoi ! »

Albert Einstein

Table of content

Introduction

Introduction

Brucellosis

Brucellosis is an infectious disease known for being one of the most widespread anthropo-zoonosis worldwide. In fact, brucellosis can be found in many different types of mammals, including cattle, goats, swine, sheeps, dogs, marine mammals, and also humans as accidental hosts (Moreno & Moriyon 2006) (von Bargen *et al.* 2012).
Human brucellosis, also called Malta fever, was first discovered by Dr. David Bruce during the second half of the 19th century on Malta Island. Symptoms may vary, depending on the infected species. In fact, cattle infection mainly results in spontaneous abortion of pregnant females and arthritis, while in humans, canonical signs of infection include flu-like symptoms such as undulant fever, headache, weakness and sweating (Moreno & Moriyon 2006). Most importantly, if not treated properly, the disease can evolve and reach a life-persisting chronic state mainly associated with heavily impairing joint and muscle pain, and may eventually lead to death (Moreno & Moriyon 2006) (von Bargen *et al.* 2012).

Regarding means of infection, it has been observed that human to human transmission of brucellosis is fairly rare. In fact the main route of human contamination has been shown to be the consumption of unpasteurized milk or dairy products obtained from infected animals (Moreno & Moriyon 2006) (von Bargen *et al.* 2012).

The anthropo-zoonotic nature of the disease has major implications regarding its control at the biological community level. In fact, the majority of the pathogenic biomass is present in animal reservoirs, while the human body only constitutes a somewhat accidental hosting organism. Additionally, it should be noted that, despite numerous attempts, no efficient human vaccine has been developed so far (Moreno & Moriyon 2006), thus resulting in the absence of any prophylactic treatment. Consequently, the systematic use of remedial treatments in human brucellosis (i.e. combination of rifampicine and doxycycline) is highly unlikely to result in eradicative outcomes (Moreno & Moriyon 2006).

For these reasons, brucellosis is considered as a major pathological threat, also referred as a bioterrorism agent, as it can severely affect society at both economical and public health levels (Moreno & Moriyon 2006) (von Bargen *et al.* 2012).

Brucella, the causative agent

Brucellosis is an infectious disease caused by bacteria from the *Brucella* genus. This genus regroups different species exhibiting an infectious potential towards a wide range of mammals while displaying typical host preferences. For example, *Brucella abortus*, the causative agent of bovine brucellosis, and *Brucella melitensis*, the causative agent of caprine brucellosis, are also able to infect humans (von Bargen *et al.* 2012). So far, ten species of *Brucella* have been discovered and named after their preferential hosts. Among these species,

Figure 1

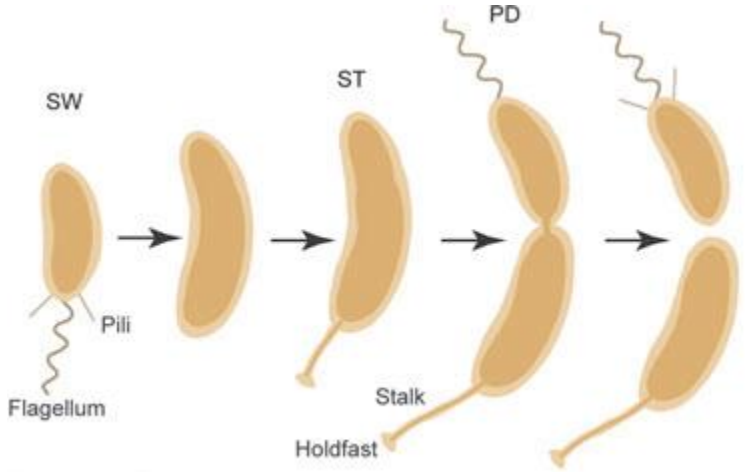

Schematic overview of *C. crescentus* cell cycle highlighting the generation of two morphologically and functionally different sibling cells. SW: swarmer cell, ST: stalked cell, PD: pre-divisional (Skerker *et al.* 2004).

Figure 2

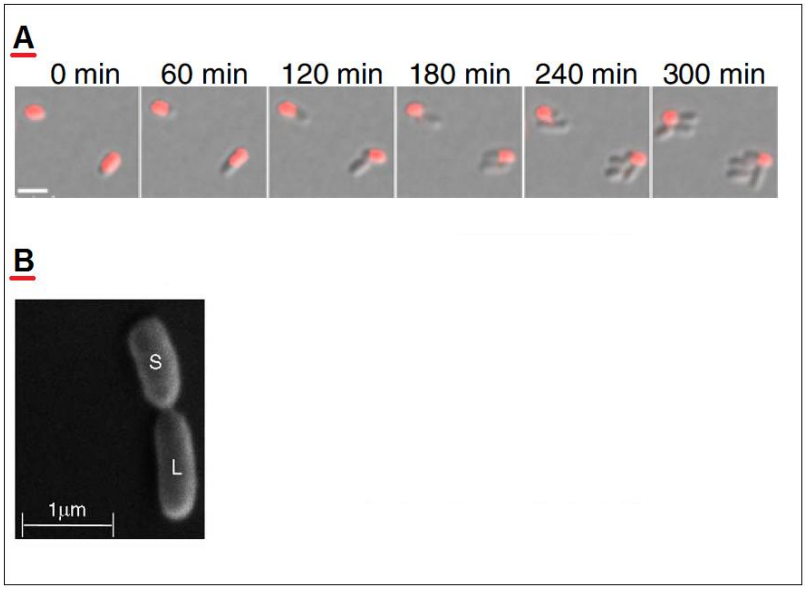

A) Differential Interference Contrast (DIC) time lapse imaging of wild-type *B. abortus* labeled with Texas Red Succinimidyl Ester (TRSE), highlighting *B. abortus* unipolar growth (red: TRSE-labeled cell wall or non-growing pole) (Brown *et al.*, 2012). The growing pole incorporates non-labeled material, allowing its easy identification compared to the non-growing (old) pole, which remains labeled with conjugated Texas Red.

B) Scanning electron micrograph of a of wild-type *B. abortus* highlighting its asymmetrical division (S: small sibling cell, L: large sibling cell). (Hallez *et al.* 2004)

three of them (*Brucella melitensis, B. abortus,* and *B. suis*, infecting caprine, bovine, and swine respectively) are known for displaying high pathogenicity towards humans, while human pathogenicity of other species is either low or undescribed (von Bargen *et al.* 2012).

Brucella spp. are small non-motile Gram negative coccobacilli belonging to the alpha-proteobacteria class, such as the cell differentiation model bacterium *Caulobacter crescentus* with which they share several features (Hallez *et al.* 2004).

In fact, it has been observed that *C. crescentus* cell cycle involves two distinct cell types, or sibling cells, which are both morphologically and functionally different (see figure 1) (Skerker *et al.* 2004). First, a non-replicating flagellated cell called the swarmer cell swims and explores its environment until finding a suitable niche to enter cell cycle. Once this niche has been found, the swarmer cell enters a specific developmental stage in order to transform into a non-swimming substrate-anchored cell type called the stalked cell. Then, this stalked cell enters cell cycle and eventually divides asymmetrically, generating a new swarmer cell while conserving the stalked cell. We can thus distinguish two morphologically and functionally different cell types. First, the swarmer cell, acting like an "explorer" searching for an appropriate replication niche, and second, the stalked cell, acting like a stationary "cell factory" actively generating new swarmer cells (Skerker *et al.* 2004).

Interestingly, this global scheme also appears to be present in *B. abortus*. In fact, recent data highlighted the fact that *B. abortus,* along with other members of the alpha-proteobacteria class, share both unipolar growth (Brown *et al.,* 2012) (see figure 2.A) and asymmetrical division (Hallez *et al.* 2004) (see figure2.B). Most importantly, this asymmetrical division event, as in *C. crescentus,* appears to give rise to functional asymmetry. In fact, it has been observed that, during infection of HeLa cells, the majority of internalized bacteria seem to belong to the small cell-type (C. Van der Henst, unpublished) (see "Functional asymmetry in infection").

Deeper into the phylogenetic tree, the *Brucella* genus belongs to the Rhizobiales order, such as plant pathogens form the *Agrobacterium* genus, or plant symbionts from both *Rhizobium* and *Sinorhizobium* genera. Interestingly, the *Brucella* genus, along with phylogenetically close genera, displays complex host-associated interactions, referred in this work as "social interactions".

For example, bacteria from the *Agrobacterium* genus such as *Agrobacterium tumefaciens* genus display pathogenic interactions with a wide range of dicotyledons. *A. tumefaciens* infection is characterized by a typical tumor induction phenomenon, known as the crown gall disease (Smith & Townsend *et al.* 1907). The infection cycle starts off with a wounded plant which, due to its tissue damages, releases several specific phenolic compounds recognized by the bacterium as chemotactically attracting signals. Once on the wound site, the bacterium will excise a specific ssDNA fragment called the T-DNA from its Ti plasmid and will transfer it inside the plant cell using a type IV secretion system called VirB. Once inside the nucleus, T-DNA encoded genes will be expressed, resulting in the synthesis of both plant hormones and specific compounds called opines. Plant hormones produced in that manner, such as auxin and specific cytokinins, will induce host hormonal deregulation, resulting in chaotic cell divisions, and thus to the formation of plant tumors. Collectively, tumorous plant

cells will also produce opines, chemical compounds which will be specifically used by the bacterium as both carbon source and nitrogen source, and as chemical signal promoting conjugation and transfer of the entire Ti plasmid form on bacterium to another (Pitzschke & Hirt, 2010).

Another example of "social interactions" originates from the *Rhizobium* and *Sinorhizobium* genera, which display typical legume symbiosis. In order to reach this symbiotic state, bacteria first invade legume root hair cells and form an infection thread allowing them to get access to the inner part of the root. Then, after infection of cortical cells, bacteria enter a specific developmental stage in order to transform into bacteroids, a modified bacterial state allowing atmospheric nitrogen fixation, therefore supplying the host with ammonia while taking advantage of its carbon source (Haag *et al*. 2012).

Here, due to their pathogenic nature, *Brucella spp* appear to share similarities with these "social interactions" patterns, but in a very specific way. In fact, due to its ability to survive in the environment, replicate in a test tube, and infect healthy animals, *Brucella spp* were initially classified as facultative intracellular pathogens (Corbel & Brinley-Morgan 1984). However, it has recently been postulated that this classification could be incorrect. In fact, it has been observed that *Brucella* preferred replication niche was the host cell intracellular environment itself, instead of the *ex-infectio* condition. Therefore, it has been postulated that a better *Brucella* life cycle classification would be a "facultatively extracellular, intracellular pathogen" (Moreno & Moriyon 2006), for which the environmental/soil phase would only constitute an obligatory stress phase conducted in order to allow dissemination from one host to another. Based on this idea, one can interpret facts regarding *Brucella* life cycle as following. First, bacteria are present in the environment, in which they are able to survive for extended periods of time ranging from several days to several months, mainly depending on temperature and sun exposure (Moreno & Moriyon 2006). Then, some of these bacteria are ingested and are able to penetrate several types of mucosal tissues. Eventually, bacteria are taken up by phagocytic cells and reach lymph nodes from which they can spread in a systemic manner (von Bargen *et al.* 2012). Once the host has been colonized, bacteria trigger their own environmental dissemination through various mechanisms, one of the main one being the abortion of pregnant females, inducing the environmental release of a heavily contaminated fetus, containing up to 10^{10} bacteria per cm^3 of fetal tissue (Moreno & Moriyon 2006).

The recent conceptual considerations listed above allow us to highlight new links between *Brucella* life cycle and host association patterns of other alpha-proteobacteria. In fact, as in the symbiotic *Rhizobium* and *Sinorhizobium* genera, *Brucella* is able to enter healthy host organisms through invasion of specific tissues and to carry out replication inside them (Moreno & Moriyon 2006). Additionally, as in the pathogenic *Agrobacterium* genus, *Brucella* is able to take control of host endogenous machineries, such as its host intracellular trafficking machineries, in order to promote its own replication by reaching its niche (von Bargen *et al.* 2012).

Figure 3

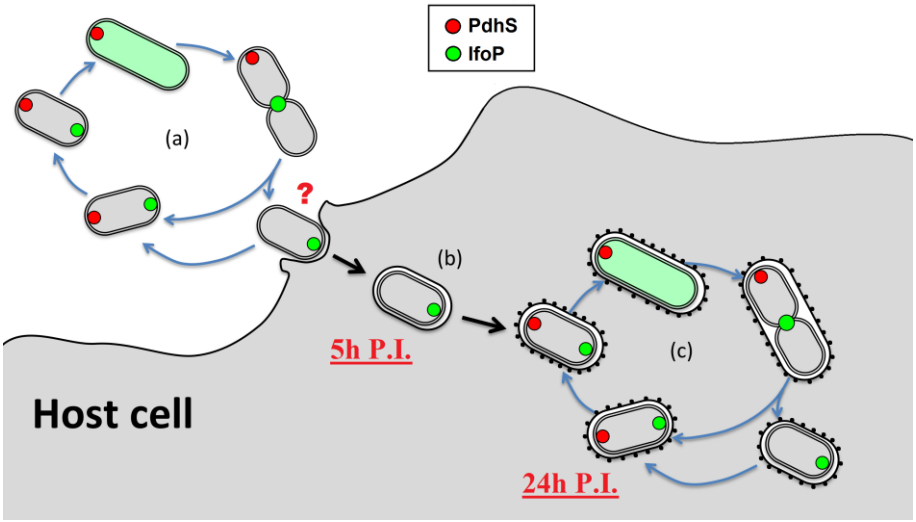

B. abortus hypothetical life cycle described using the PdhS (red) and IfoP (green) as polar markers highlighting in a) *B. abortus* environmental/*in vitro* cell cycle, b) *B. abortus* as observed 5 hours post infection (P.I.) displaying the recurrent PdhS-/IfoP+ phenotype, c) *B. abortus* as observed 24 hours P.I. displaying active cell division in its ER-derived replication niche.

Brucella abortus cell-level infection

In this work, we have chosen to focus on *Brucella abortus*, the *Brucella* species responsible for bovine brucellosis. At the cellular level, *B. abortus* infection implies numerous interactions with specific host cell targets through the use of diverse mechanisms, many of which are still unknown today (Moreno & Moriyon 2006) (von Bargen *et al.* 2012).

So far, it has been observed that, in both professional and non-professional phagocytes, *B. abortus* first enters eukaryotic cells through the endosomal pathway. However, based on protein markers analysis, it has been observed that the composition of this endosome quickly shifts in order to become a specific intracellular compartment called the BCV (Brucella Containing Vacuole) which undergoes a complex maturation process (von Bargen *et al.* 2012). In fact, it has been shown that BCVs first interact with compartments of the early endocytic pathway, thus acquiring specific markers such as Rab5 and EEA1 (von Bargen *et al.* 2012). Then, such markers are progressively lost and BCVs obtain the typical lysosomal marker LAMP1 (Frenchick *et al.* 1985). In non-professional phagocytes such as HeLa cells, most BCVs are able to reach the endoplasmic reticulum while only a few are addressed to the phagolysosome for degradation (Moreno & Moriyon 2006) (von Bargen *et al.* 2012). In professional phagocytes however, most of the BCVs eventually fuse to lysosomes, leading to the formation of bacteria-degrading phagolysosomes, while only a few vesicles are able to prevent lysosomal fusion and to reach their dedicated endoplasmic reticulum replication niche through unknown mechanisms (von Bargen *et al.* 2012). It should be noted that the fusion of BCVs to the endoplasmic reticulum appears to be depending on the presence of ERES (Endoplasmic Reticulum Exit Sites), as it has been observed that the disruption of these sites prevents BCV fusion and thus prevents bacterial replication (Celli *et al.* 2005).

Functional asymmetry in infection

Recent studies conducted in our laboratory have characterized *Brucella abortus* replication cycle in HeLa cells. It has been observed that *B. abortus* infection is characterized, at the cellular level, by two distinct phases. First, a "lag-phase", consecutive to host cell internalization and characterized by the absence of detectable bacterial proliferation, followed by a second "proliferation phase" characterized by massive bacterial division inside ER compartments. Most importantly, it has been showed using fluorochrome-coupled polar markers (PdhS, an essential histidine kinase of unknown function, and IfoP, a protein of unknown function) that, a few hours post-infection, only the small bacterial cell type was observed inside infected eukaryotic cells during the "lag phase" (see figure3.B), as opposed to the "proliferation phase" during which both bacterial cell types are present (typically 24h post-infection) (Van der Henst, unpublished) (see figure3.C). Consequently, it has been suggested that this small cell type, displaying a PdhS-/IfoP+ phenotype, could be the only one capable of infecting eukaryotic cells. Moreover, due to the fact that, as opposed to the *in infectio* "lag phase", bacteria from the small cell type (PdhS-/IfoP+) are very transient during

the *in vitro* cell cycle (Hallez *et al.* 2007), we hypothesized that these cells could be subjected to a **systematic cell cycle blockade**, possibly remaining in such a state during most of the trafficking process, until reaching the endoplasmic reticulum.

However, the loss of the polar PdhS focus could be simply the consequence of bacterial internalization (e.g. due to signals directly or indirectly sensed by this histidine kinase), meaning that the *in infectio* PdhS-/IfoP+ bacteria would be very different from those characterized in rich culture medium, and thus could possibly not be blocked in their cell cycle. Therefore, the systematic preservation of **the PdhS-/IfoP+ phenotype a few hours post-infection cannot be straightforwardly connected to a cell cycle blockade**.

It should be noted that, during infection of HeLa cells, two parameters greatly impair any large scale analysis of invading bacteria: on the one hand, the proportion of eukaryotic cells infected, and on the other hand, the number of invading bacteria per infected eukaryotic cells. In fact, as observed in our team, the number of eukaryotic cells infected is intrinsically very low, typically of about 5%. In addition, the number of invading bacteria for a given HeLa cell is very low as well, typically ranging from 1 to 2 bacteria per eukaryotic cell (for a bacteria over eukaryotic cell ratio of 300).

Cell cycle and chromosome replication in bacteria

The duplication of the genetic information and its equal distribution among daughter cells is an essential cell cycle hallmark.

In eukaryotic cells, cell cycle is divided into four distinct steps: the G1 phase, the S phase during which genetic information is being duplicated through DNA synthesis, the G2 phase, and finally the M phase which includes prophase, anaphase, metaphase, telophase and cytokinesis.

In prokaryotic cells however, such phases are not observed because growth and chromosome replication occur simultaneously. In fact, only three cell cycles phases have been characterized, based on the replication state of the chromosome(s). First, the B period, which spans from cell birth to the initiation of chromosome replication, second, the C period, which is established between chromosome replication initiation and termination, and finally, the D period, which begins at chromosome replication termination and ends at cell division (Rasmussen *et al.* 2007). In most prokaryotes, chromosome replication starts bidirectionally from a unique site called the origin of replication (*oriC*) and ends at the terminus site (*terC*), which is located at about 180° away from the *oriC* considering a circular chromosome. Origin and terminus sites are functionally and structurally defined. Typical *oriC* sites contain at least one DnaA box (see below), usually flanked by genes involved in chromosome replication, and are characterized by a low GC content segment proposed to favor DNA unwinding (Zakrewska *et al.* 2007). The nature of termini regions remains less clear, but in *Escherichia coli*, *terC* site contains several replication pause sites, recognized by specific terminator proteins, and separated into two groups organized head-to-head towards the center of the terminus region, forming a so called “replication fork trap” (Duggin & Bell 2009).

Initiation of replication mainly involves the key protein DnaA, and more precisely the binding of its active form (or ATP-bound DnaA) on the *oriC* (onto a 9 bp sequence called DnaA box). Once bound, this highly conserved ATPase is able to unwind double-stranded DNA, therefore allowing access to other proteins of the replication machinery, such as DnaB and DnaC (helicase and helicase regulator protein, respectively) (Kaquni 2012). Additionally, DnaA has been showed to directly interact with several structuring DNA-binding proteins (such as the histone-like proteins Fis and IHF), and can also act as a transcription factor regulating the expression of genes involved in chromosome replication (Zakrewska *et al.* 2007).

In slowly growing bacteria, chromosome replication occurs only once per cell cycle. In fact, as implied by the nature of the BCD phases, chromosome replication and cell cycle appear to be deeply linked among prokaryotes (Mierzejewska & Jaqura-Burddzy 2012). For example, it has been known for long that, in *B. subtilis*, cell division is inhibited as long as the chromosome is not segregated due to its nucleoid occlusion system (Harry 2001). More recently, it has been shown in *Caulobacter crescentus* that MipZ, an ATPase which associates with the chromosome partitioning system, was able to prevent FtsZ ring formation until the newly synthesized chromosomes reach their respective cell halves (Schofield *et al.* 2010). Moreover, it has been found that a specific defect in *C. crescentus* chromosome partitioning protein ParB (see below) leads to a switch in the ADP/ATP-bound ParA ratio (see below), inducing an inhibition of the cell cycle (Figge *et al.* 2003).
Based upon these facts, it seems rather clear that cell cycle and chromosome replication are closely connected in bacteria. Therefore, one can assume that **it is possible to determine the cell cycle state of a given bacterium by investigating its chromosome replication status**, which may be done **by visualizing and following the duplication and segregation dynamics of its *oriC* and *terC* regions**.

B. abortus genome and chromosome synchronicity

Unlike model bacterium such as *B. subtilis*, *E. coli* or *C. crescentus*, *B. abortus* has a genome divided into two single copy circular chromosomes of different sizes, first a 2.12 Mb chromosome (or chromosome I), and second a 1.16 Mb chromosome (or chromosome II) (Halling *et al.* 2005). The two chromosomes are thought to have different evolutionary origins. In fact, it has been shown in *B. suis* that chromosome I possesses typical chromosome partitioning proteins widely distributed among other alpha-proteobacteria (see "chromosome segregation" section below), while chromosome II possesses a typical plasmid-like segregation system (see "chromosome segregation" section) (Paulsen *et al.* 2002). Moreover, chromosomes display a deep asymmetry regarding functional categories of genes they encode. For example, chromosome I possesses the majority of genes involved in transcription, translation, and protein synthesis, while chromosome II possesses genes involved in membrane transport, central intermediary and energy metabolism, and associated regulation

(suggesting auxiliary pathways for the use of specific substrates) (Paulsen *et al.* 2002). Additionally, it should noted that chromosome II also encodes potential virulence factors such as the type IV secretion system *virB* operon and genes involved in flagellar biosynthesis (Paulsen *et al.* 2002).
Based upon these facts, it has been postulated that chromosome II is likely to have evolved from an ancestrally acquired megaplasmid. However, it should be noted that this acquisition event could have occurred quite anciently, knowing that the overall GC content of each chromosome is very similar (about 57%), therefore suggesting long term nucleotide adaptation (Paulsen *et al.* 2002) (Moreno & Moriyon 2006).

Compared to conventional mono-chromosomal bacterial species, the fact of possessing a multipartite genome addresses new questions. In fact, having to deal with two chromosomes of different size necessitates the ability to somehow coordinate two different and possibly simultaneous replication and segregation events in order to generate a viable descent, therefore adding a supplementary level of complexity.
So far, no information regarding any chromosome replication synchrony in *B. abortus* has been brought to light. However, this coordination issue has already been extensively investigated in the pathogenic model bacterium *Vibrio cholerae*. In this model, which also possesses a genome made of two circular chromosomes of different sizes, it has been observed that chromosome II replication is delayed compared to chromosome I in such a way that both replication events roughly terminate at the same time (Rasmussen *et al.* 2007). Based on these facts, it is possible to imagine several plausible chromosome replication models for *B. abortus*, such as a termination-based "*Vibrio*-like dynamic", an opposite initiation-based dynamic, or possibly a completely different model involving other points of regulation.

Chromosome segregation

Robustness is an essential trait of the transmission of genetic information from one organism to its offspring regarding life as a whole. At the molecular level, faithful chromosomal segregation is fundamental to generate a sustainable progeny. For that reason, one can easily understand that having such processes governed by a flawed system or even pure randomness would constitute a major defect, which would eventually be counter selected at the evolutionary level. Therefore, several mechanisms have been selected in order to allow an accurate and reliable transmission of the genetic information.
In eukaryotic cells, the loosely condensed DNA-protein complex or euchromatin is first replicated during S-phase, and then turned into a highly condensed structure or heterochromatin which constitutes the actual chromosomes. After nuclear envelope dismantlement, microtubules from the mitotic spindle bind every sister chromatid centromere thanks to a ring-shaped protein complex called kinetochore (Tomoyuki 2010). Then, sister chromatids are separated from one another and pulled apart towards the opposite cell poles, during anaphase, due to microtubules depolymerization in such a way that each pole receives

Figure 4

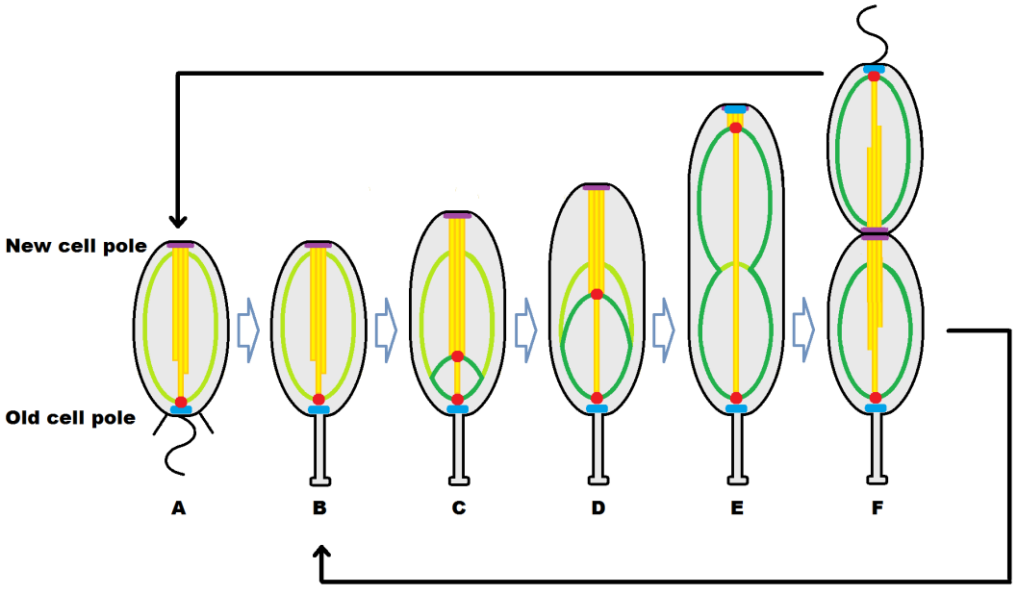

C. crescentus cell cycle, highlighting the role of the *parS*/ParB/ParA system in chromosome segregation. Chromosome before replication is shown in light green, the replicated chromosomal regions are shown in dark green. A) In a flagellated (swarmer) cell, ParB-bound *parS* (red) interacts with a few ParA filaments (yellow) while anchoring the chromosome (light green) at the old cell pole by interacting with PopZ (blue). At the new pole, TipN (purple) is thought to affect ParA filament stability (Mackiewicz *et al.* 2004). B) The flagellated cell differentiates into a stalked cell, ParB-bound *parS* is released from the old pole. C) The stalked cell grows, chromosome replication is engaged and ParA filaments bind the neosynthesized ParB-bound *parS* complex. D) The depolymerization of ParA filaments generates a force which pulls a copy of the duplicated chromosome (dark green) towards the new cell pole. E) PopZ also accumulates at the new pole before the end of the ParB-*parS* complex migration in order to anchor the duplicated chromosome by interacting with its ParB-bound *parS* complex. F) Chromosome replication and the synthesis of a new flagellum at the initial "new pole" are both terminated, ParA filaments are rearranged and TipN relocalizes at the constriction site.

Figure 5

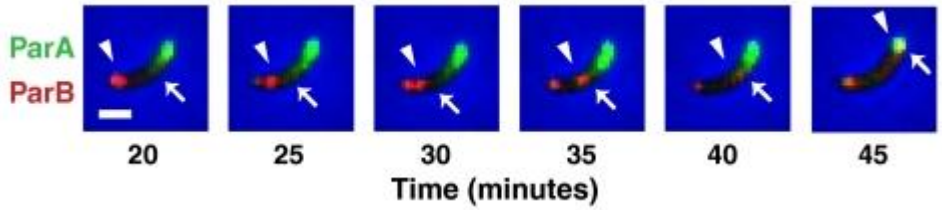

Time lapse imaging of *C. crescentus* showing the distribution of chromosome segregation proteins ParA (green) and ParB (red) over time, highlighting the ParA structure retraction resulting in the pulling of newly generated ParB focus towards the opposite cell pole. (Shebelut *et al.* 2010)

an equal set of duplicated chromosomes (Tomoyuki 2010). Once each set has reached its specific pole, the two nuclear envelopes are reformed and the cell can start cytokinesis.
In prokaryotic cells, chromosomal segregation remains poorly understood. Nevertheless, a series of recent discoveries suggested the existence of different species-specific mechanisms for chromosome segregation. For example, in *E. coli*, it has been proposed that, due to the apparent absence of chromosome-partitioning proteins, chromosome segregation could be achieved by cause of ejection of the neo-synthesized DNA away from the replication machinery towards cell poles (Lemon & Grossman 2001). Moreover, this first mechanism could possibly be coupled to an entropy increase due to a conformational relaxation obtained after strand separation from the compacted nucleoid (Jun & Wright 2010). However, several bacterial species such as *B. subtilis*, *V. cholerae*, and *C. crescentus*, possesses a functionally homologous chromosome segregation machinery known as the ***parABS*** system (Toro & Shapiro, 2010), also called spindle-like apparatus, comparable to the eukaryotic segregation system (Toro *et al.* 2008) (see below).

Up to now, no information regarding *B. abortus* chromosome segregation machineries could be found in the literature. Moreover, similar data regarding phylogenically close bacteria such as members of the *Agrobacterium, Rhizobium* and *Sinorhizobium* genera are still missing. However, our team recently identified two putative chromosome-specific segregation systems which are presently in course of characterization (Deghelt *et al.* unpublished).

Based on these results, chromosome I partition is thought to be ensured by a highly conserved *C. crescentus*-like *parABS* system (Toro *et al.* 2008). In this system, a chromosomal centromere-like sequence (*parS*) is first specifically recognized by the DNA-binding protein ParB (Easter & Gober, 2002) (Mohl & Gober, 1997). Then, ParB is recognized by ParA, a filamentous polymer-forming protein anchored at the new cell pole. When chromosome segregation is engaged, ParB-bound ParA filaments start depolymerizing. This depolymerization event leads to the retraction of the ParA cloud, thus generating a force pulling one of the two neo-synthesized *oriC* towards the new cell pole (see figure 4).
It should be noted that several studies already aimed at localizing components of the *parABS* system intracellularly, such as in *C. crescentus* (Mohl & Gober, 1997) (see figure 5), showing that ParB localization follows the same dynamic than the *C. crescentus ori* (Viollier *et al.* 2004). In *B. abortus* however, no such intracellular localization have been found in the literature. Nonetheless, our team recently succeeded at monitoring ParB localization during *B. abortus* in vitro cell cycle, highlighting a *Caulobacter*-like polar distribution of ParB foci (Deghelt *et al.* unpublished) (see figure 6).

Chromosome II partition is thought to be ensured by the *repABC* operon, a low copy plasmid segregation system commonly found among Rhizobiales such as in the *Agrobacterium* (Ti plasmid), *Rhizobium* (p42d plasmid), and *Sinorhizobium* (pSymA plasmid) genera (Winans *et al.* 2012). Up to now, the molecular mechanism of this system remains poorly understood, but it appears that RepA and RepB (distant homologs and functional analogs of ParA and ParB, respectively) are directly involved in plasmid segregation through interaction with a chromosomal *parS*-like sequence (*repS*) and in self negative regulation at the transcriptional level (Cevallos *et al.* 2008). Furthermore, recent

Figure 6

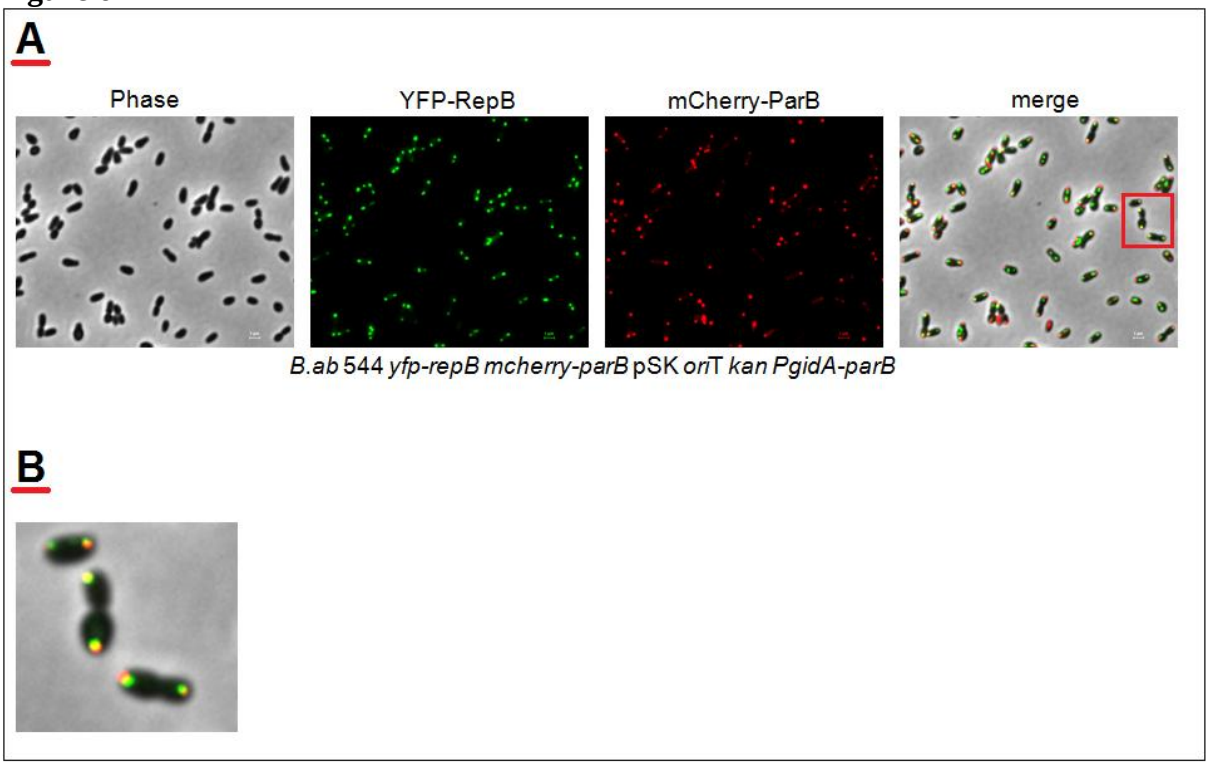

A) Intrabacterial localization of YFP-RepB (green) and mCherry-ParB (red) in a strain of *B. abortus* having an additional copy of *parB* under the control of the *gidA* promoter. The bacteria are detected by phase contrast. In the merge panel, the red square is delimiting the inset shown in B.

B) Inset showing the systematic colocalization of the two fusion proteins YFP-RepB and mCherry-ParB. (M. Deghelt, unpublished)

Figure 7

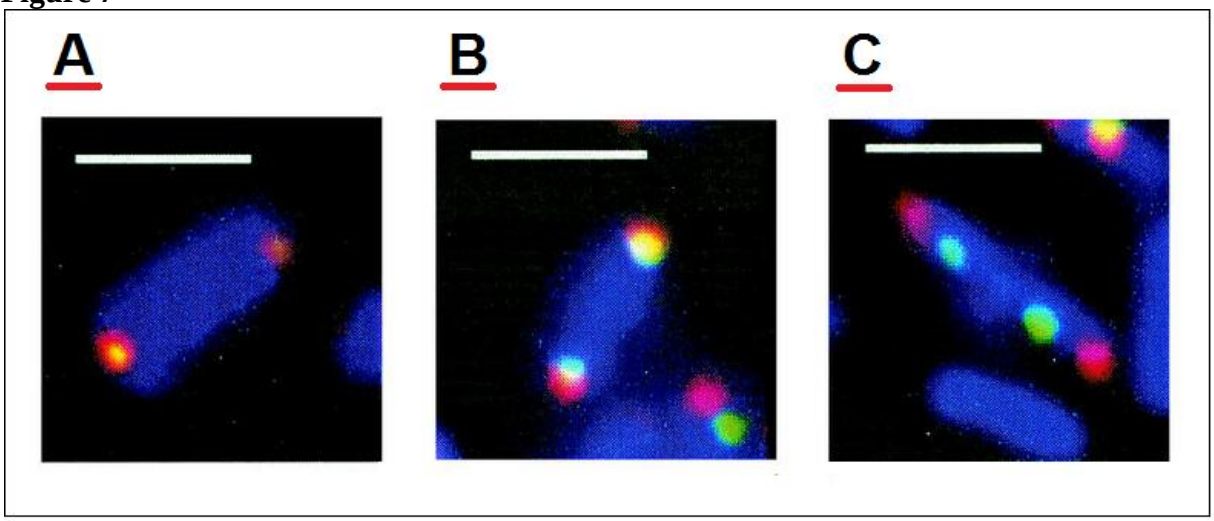

Fluorescence *In situ* Hybridization (FISH) analyses in *A. tumefaciens* showing in A) dual labeling of the origin of replication of the circular chromosome (red + green), B) circular chromosome *ori* –labeling (red) and linear chromosome *ori*-labeling (green), C) circular chromosome *ori* –labeling (red) and Ti plasmid *ori*-labeling (green). (Blue: genome/nucleoid DAPI staining) (Kahng & Shapiro 2003).

studies have gathered evidences suggesting that RepC would act as a DnaA-like functional analog as it appears to initiate chromosome II replication (Cervantes-Rivera *et al.* 2011). In fact, it has been observed that, in alpha-proteobacteria possessing one or several *repABC* replicon(s), the overexpression of RepC induced an increase in the replicon copy number. Interestingly, this increase in copy number only affects the replicon from which RepC had been overexpressed. Consequently, it has been suggested that RepC only displays a strict *cis* specificity for the replication initiation control, therefore allowing the co-existence of several *repABC* replicons, even if sharing extremely high RepC protein identity (up to 97% between two *repABC* replicons in *Rhizobium etli*) (Winans *et al.* 2012). The fact of replicating the *repABC*-based replicon only once per cell cycle implies the ability to accurately repress the operon expression. Following this idea, it has been observed that, besides their primary function in replicon segregation, both RepA and RepB were also able to bind to the *repABC* operon promoter, resulting in autorepression (Winans *et al.* 2012). Moreover, it has been observed that the transcription of RepE, a small anti-sense non-coding RNA transcribed from the region located between *repB* and *repC*, is able to hybridize onto *repC* mRNA, resulting in both transcriptional and translational inhibition of *repC* (Winans *et al.* 2012).

Most importantly, besides the work that has been performed in our team (intracellular localization of chromosome II partitioning protein RepB) (see figure 6) (Deghelt *et al.* unpublished), no specific localization of the *repABC* proteins has been realized so far. However, closely related experiments used FISH analysis in order to simultaneously localize endogenous *repABC*-based replicons and origins of replication of circular chromosomes in *A. tumefaciens* and *S. meliloti* (Kahng & Shapiro 2003). In this study, chromosomal *ori* adopted a strictly polar localization, whereas *repABC*-based replicons were located close to the cell poles, typically ranging from chromosomal *ori*-neighboring patterns to quarter-cell positioning, depending on the investigated replicon (see figure 7) (Kahng & Shapiro 2003).

Cell cycle blockade and its investigation

As stated above, one of the most intriguing features about *B. abortus* host cell invasion process is its apparent cell cycle blockade observed during several hours post-infection, where bacteria majorly display a PdhS-/IfoP+ phenotype. However, the likely absence of direct correlations between previously used polar makers (PdhS/IfoP) and bacterial cell cycle requires the use of other investigation techniques in order to test the absence of DNA replication.

A possible strategy could be to use *B. abortus* endogenous chromosome partitioning proteins fused to specific fluorescent proteins in order to intracellularly localize both *ori*s in living cells. Two fusions had already been constructed by our team; first, mCherry-ParB, putatively recognizing chromosome I origin of replication, and YFP-RepB, putatively recognizing chromosome II origin of replication. The bottom-line of this strategy is to postulate that, by following the number of foci of a given fluorescent protein, one can approximate the number of associated *ori*, and thus one can propose that replication has started for a given chromosome. Such fusion genes have already been constructed and placed

Figure 8

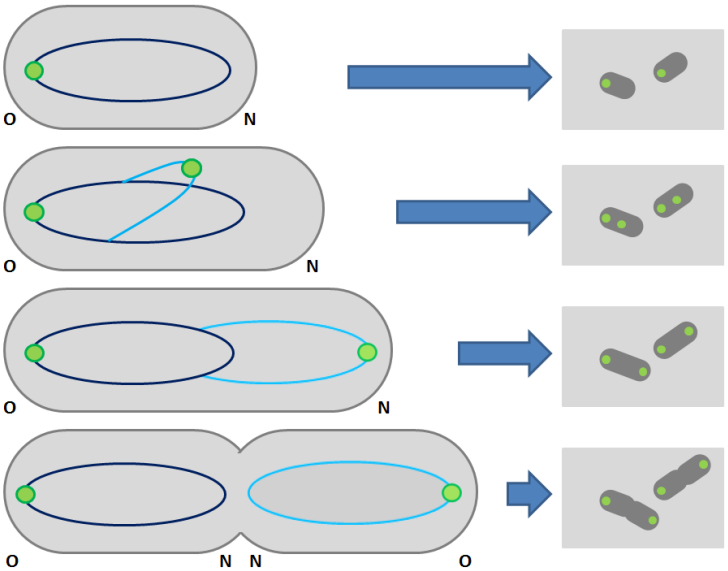

Schematic representation of bacterium displaying a *parS*-labeled *ori* region specifically recognized by a hypothetical green fluorescent fusion protein along cell cycle (left) with hypothetical phenotypes as observed under the microscope (right). (Dark blue: initial copy of the chromosome, light blue: actively segregated copy of the chromosome, O: old pole, N: new pole).

in *B. abortus* 544 genome by allelic replacement (Deghelt *et al.* unpublished). The expression of these two fusions revealed foci distribution patterns similar to those observed in *C. crescentus* for chromosome I and similar to *A. tumefaciens* and *S. meliloti* associated plasmids (Kahng & Shapiro 2003) for chromosome II (Deghelt *et al.* unpublished). However, even though promising, this strategy is also characterized by a major weakness. In fact, this method only allows **indirect** visualization of the intracellular position of both *ori*s thanks to their putative DNA-binding proteins. Consequently, even though the recognition of *parS* by ParB and *repS* by RepB is presently being demonstrated in *E. coli*, there is no evidence that the foci observed with this method literally match the *ori*s in *B. abortus*.

Consequently, we decided to conduct a strategy similar to the one exposed in Li *et al.* 2002, in which small exogenous DNA sequences are specifically inserted at chromosomal locations of interest before being specifically recognized by fluorochrome-coupled DNA-binding proteins. According to the strategy described in Nielsen *et al.* 2006, two different systems will be used; on the one hand, the "**P1 system**", derived from *E. coli* bacteriophage P1 partitioning system, and on the other hand, the "**pMT1 system**", derived from *Yersinia pestis* virulence plasmid pMT1 partitioning system. Each of these systems includes a specific *parS* sequence (either ***parS* P1** or ***parS* pMT1**, depending on its origin) which is recognized by its associated DNA-binding protein (either **ParB P1** or **ParB pMT1**, depending on its origin) fused to specific fluorescent proteins (**CFPEc**, displaying a CFP-like spectrum, and **yGFP**, displaying an YFP-like spectrum). The way these systems work is the following. First, *parS** (being either *parS* P1 or *parS* pMT1) is inserted at a chromosomal location of interest through allelic replacement. Then, the bacterium is transformed in order to obtain a plasmid carrying the gene coding for the associated fusion protein XFP-ParB* (being either **CFPEc-ParB P1** or **yGFP-ParB pMT1**). Then, as for the mCherry-ParB YFP-RepB approach, the idea is to correlate the number of observed foci for a given fluorochrome with the replication state of the associated chromosome, depending on the location of the *parS** sequence (see figure 8). Moreover, not only the origins but also the termini regions (or potentially any other chromosomal region) can be targeted using this method, therefore allowing us to monitor chromosome replication termination, since the chromosomal insertion of *parS** is only directed by specific allelic replacement.

It should be noted that no crosstalk has been observed between the P1 and pMT1 system in *E. coli* (Nielsen *et al.* 2006) and *C. crescentus* (Toro *et al.* 2008), and that, in *C.* crescentus, no interference with its endogenous *parABS* segregation system has been observed (Toro *et al.* 2008). Additionally, both *parB* P1 and *parB* pMT1 sequences have been specifically truncated in order to only conserve their DNA-binding domain (resulting in the removal of the 30 first amino acids of *parB* P1 (Li *et al.* 2002) and the 23 first amino acids of *parB* pMT1 (Nielsen *et al.* 2006)), thus getting rid of the potentially interfering ParA-interacting domain (Nielsen *et al.* 2006).

Objectives

Objectives

As stated in the introduction, the study of *B. abortus* cell cycle in infection, using PdhS and IfoP as polar markers, highlighted a potential cell cycle blockade typically lasting for several hours post infection and characterized by a PdhS-/IfoP+ phenotype.

The main goal of this work was to characterize *B. abortus* cell cycle and more specifically the replication status of this bacterium in the non-proliferative stage of the infection in epithelial cells. To achieve this goal, we needed to construct tools (which first had to be validated in bacteriological culture) able to report chromosome-specific replication status at the single cell level. We chose to construct *B. abortus* strains carrying small exogenous DNA sequences, referred as *parS** sequences (being either *parS* P1 or *parS* pMT1), inserted at specific chromosomal loci (***ori*I**, ***ter*I**, ***ori*II**, ***ter*II**, and the ***dnaA*** locus) through allelic replacement. Then, using specific fluorochrome-coupled *parS**-binding proteins, referred to as XFP-ParB*, we expected to monitor the number and the localization pattern of each fluorochrome-specific foci and correlate these two parameters with the intracellular localization and replication state of the associated chromosomal sites. Indeed, we expected that if a given *parS**-inserted chromosomal site was duplicated and segregated, our reporter system would display two foci, whereas in the absence of replication, only one single focus would be observed.

Validation of the proposed reporter strains will be achieved by comparing the number of chromosomal site-specific foci per bacterium in a bacterial population (obtained by microscopic analysis) to the genomic content as indicated by flow cytometry analysis. In fact, the duplication of the *ori*s-associated foci will be used as a marker of chromosome replication initiation corresponding to an either S or 2n replication status, whereas the presence of a single focus will be directly correlated with a 1n replication status. Likewise, the duplication of *ter*-associated foci will be used to monitor chromosome replication termination, correlated with a 2n replication status, whereas the presence of a single focus will be correlated with an either 1n or S replication status.

A first objective would be to characterize *B. abortus* cell cycle ***in vitro***. To begin with, we will be to analyze the number and the intrabacterial distribution of foci relative to their chromosomal insertion sites using strains carrying a single *parS** sequence at the time (referred to as **single** *parS**-carrying strains) cultured in bacteriological growth medium. Also, the distribution of these foci will be analyzed relative to the nature of the bacterial poles (growing or non-growing) using TRSE labeling (non-growing pole staining). Then, we will conduct similar analyses on strains simultaneously carrying two *parS** sequences at different chromosomal insertion sites (referred to as **double** *parS**-carrying strains). These strains should enable us to answer several biological questions by following two different approaches.

On the one hand, we will perform a chromosome-based approach, using strains for which the *ori* and the *ter* regions of a given chromosome have been simultaneously *parS**-labeled. Such strains should allow us to monitor chromosome-specific replication and

segregation dynamics by discriminating each of BCD phases for a given chromosome (one *ori* focus and one *ter* focus, two *ori* foci and one *ter* focus, and two *ori* foci and two *ter* foci, respectively). Additionally, the dual labeling of *ori* and *ter* regions should also allow us to detect possible chromosome-specific intracellular orientation patterns.

On the other hand, we will perform a replication-based approach, where we should be able to monitor the replication initiation and, separately, the replication termination of both chromosomes at the same time, using strains for which either both *ori*s or both *ter*s have been simultaneously labeled. Following this idea, these strains should also allow us to test for a possible synchronization of chromosome replication, being either initiation-synchronized (identifiable by using dual *oris* labeling) or termination-synchronized (identifiable by using dual *ter*s labeling).

A second objective would be to characterize *B. abortus* cell cycle ***in infectio*** using HeLa cells as artificial host cells. The main point of this section is to investigate the validity of the cell cycle blockade hypothesis by quantifying the number of foci corresponding to *B. abortus ori*I and *ori*II five hours post-infection, using the same strains as described in the section above.

Finally, a third objective would be to either validate or refute the previously obtained data regarding the intracellular localization of the two *B. abortus* endogenous chromosome segregation systems (Deghelt *et al.* unpublished). In fact, due to the relatively small distance between the *B. abortus* endogenous *parS*/*repS* sequences and the *ori*I/*ori*II inserted *parS** sequences at a chromosomal scale, fluorochrome-coupled ParB/RepB foci should specifically colocalize with XFP-ParB* foci. To test this hypothesis, we plan to generate a *parS**-labeled *ori*I region in a previously constructed *B. abortus* mCherry-ParB strain and express the associated plasmid-encoded XFP-ParB* fusion protein. Similarly, we plan to generate a *parS**-labeled *ori*II region in a previously constructed YFP-RepB *B. abortus* strain and express the associated plasmid-encoded XFP-ParB* fusion protein

Results

Figure 9

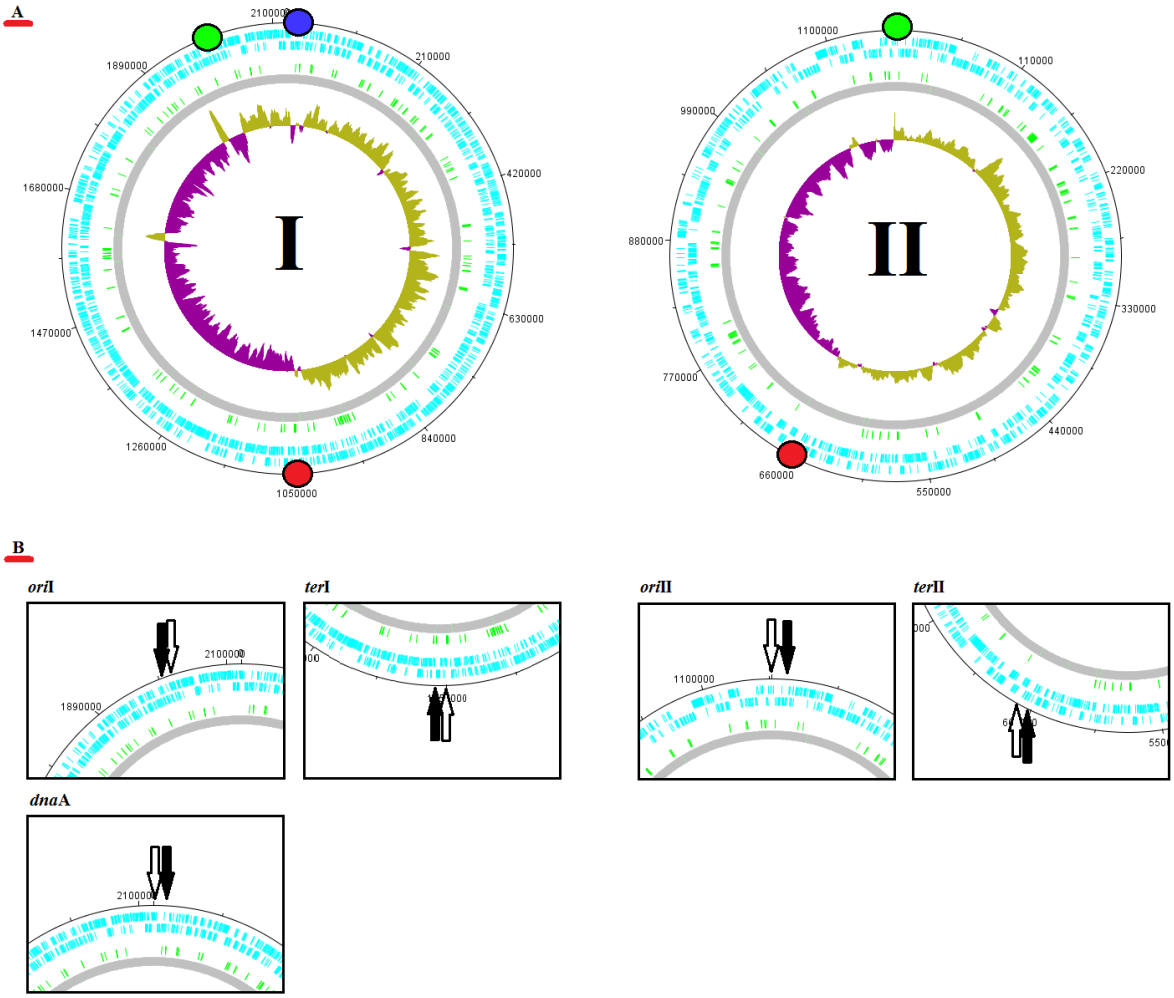

Theoretical localization of chromosomal regions of interest mapped using the "DNA plotter" software for the *B. abortus* 2308 strain genome. Blue lines represent strand specific CDS, green lines represent miscellaneous features, and the purple/yellow graph represents the calculated GC-skew for a 10kb sliding window. A) Mapping of both *ori*s (green dot) and *ter*s regions (red dot) on chromosome I (left) and II (right), as proposed by our team. The blue dot represents the *dnaA* gene, proposed to be the actual *ori* according to B. abortus 2308 genome annotation. B) Using the same scale as in figure 3.A, discrimination between actual regions (white arrows, e.g. *ori*I) and targeted regions for *parS** insertion (black arrows, e.g. *Nori*I) for each chromosomal location of interest.

Results

Identification of chromosomal regions of interest

First of all, chromosomal regions that we intended to locate have to be accurately identified. In *B. abortus* 2308 genome, the origin of replication of chromosome I and II (called *ori*I and *ori*II, respectively) have been previously approximated based on the location of the replication initiator protein genes *dnaA* and *repC*, respectively (Chain *et al.* 2005). However, we think that these reference locations could be inexact. In fact, a recent study has highlighted three parameters which could be used in order to locate prokaryotic replication origins (Mackiewicz *et al.* 2004). First, the most universal criterion is a switch in the polarity of the GC-skew (defined as (C-G)/(C+G) for a single strand of DNA, and calculated in this case for a 10kb sliding window), second, the location of DnaA boxes cluster, and finally the location of the *dnaA* gene itself (which is known to be the less universal criterion) (Mackiewicz *et al.* 2004). Consequently, we analyzed *B. abortus* 2308 genome based on these criteria, using Sanger Institute's software "DNA plotter", and identified putative *ori* regions different from those that had been previously predicted. In fact, we detected a major switch in GC-skew polarity located about 115kb away from the initial origin for chromosome I, and only about 3kb away from the initial origin for chromosome II (see figure 9.A). Moreover, we noticed that, in chromosome I, the region containing the GC-skew switch was also characterized by the presence of the *hemE* gene (as in *C. crescentus*), a region which had previously gathered evidence to house the chromosome *ori* in its promoter region (Bellefontaine *et al.* 2002). Additionally, a previous study also highlighted the presence of a cluster of three *dnaA* boxes in *Brucella suis* 1330 chromosome I (Mackiewicz *et al.* 2004). We thus analyzed this hypothetical *ori*I region, as displayed in the *B. abortus* 2308 genome sequence, using the ApE software and detected a cluster of three possible *dnaA* boxes (consensus TTATCCACA sequence, with one mismatch allowed) upstream of the *hemE* gene.

Regarding *ter* regions, it appears that, according to the GC-skew polarity switch, their locations are not exactly 180° away from the *ori*s, especially for chromosome II (see figure 9.A). We could thus hypothesize that one possible reason to explain such a shift compared to the intuitive "180° away" location could be a difference in the speed of replication between the two arms of the chromosome.

Once identified, these chromosomal regions were targeted for the insertion of an exogenous *parS** sequence (see "Insertion of *parS** into plasmids carrying chromosomal region of interest"). However, it should be noted that the regions targeted for *parS** integration are not the actual *dnaA*, *ori*s and *ter*s regions, since their alteration could possibly disrupt their function and thus generate non-viable strains. In fact, we rather chose to target **neighboring** regions (therefore named ***Nori***s, ***Nter***s, and ***NdnaA***), located close to the putative *ori*s and *ter*s (see figure9.B). Moreover, integration sites of these neighboring regions have been specifically selected in order to be located inside intergenic regions flanked with genes oriented head-to-head. In fact, these configurations should weaken the probability to

Table 1

strain name/genotype	*Nori* I	*Nter* I	*Nori* II	*Nter* II	*NdnaA*	pMR YB CB	pMR YB	pMR CB
B. ab 544 wt pMR10-kan *cfpEc-parB* P1								
B. ab 544 wt pMR10-kan *ygfp-parB* pMT1								
B. ab 544 wt pMR10-kan ygfp-parB pMT1 cfpEc-parB P1								
B. ab 544 *Nori* I *parS* P1 pMR10-kan ygfp-parB pMT1 cfpEc-parB P1	**P1**							
B. ab 544 *Nori* I *parS* pMT1 pMR10-kan ygfp-parB pMT1 cfpEc-parB P1	**pMT1**							
B. ab 544 *Nter* I *parS* P1 pMR10-kan ygfp-parB pMT1 cfpEc-parB P1		**P1**						
B. ab 544 *Nori* II *parS* pMT1 pMR10-kan ygfp-parB pMT1 cfpEc-parB P1			**pMT1**					
B. ab 544 *Nter* II *parS* pMT1 pMR10-kan ygfp-parB pMT1 cfpEc-parB P1				**pMT1**				
B. ab 544 *Nori* I *parS* pMT1 *Nter* I *parS* P1 pMR10-kan ygfp-parB pMT1 cfpEc-parB P1	**pMT1**	**P1**						
B. ab 544 *Nori* II *parS* pMT1 *Nter* II *parS* P1 pMR10-kan ygfp-parB pMT1 cfpEc-parB P1			**pMT1**	**P1**				
B. ab 544 *Nori* I *parS* P1 *Nori* II *parS* pMT1 pMR10-kan ygfp-parB pMT1 cfpEc-parB P1	**P1**		**pMT1**					
B. ab 544 *Nter* I *parS* P1 *Nter* II *parS* pMT1 pMR10-kan ygfp-parB pMT1 cfpEc-parB P1		**P1**		**pMT1**				
B. ab 544 *Nori* I *parS* P1 *NdnaA parS* pMT1 pMR10-kan ygfp-parB pMT1 cfpEc-parB P1	**P1**				**pMT1**			

parS P1	*parS* pMT1
P1	**pMT1**

pMR CB	pMR10-*kan* cfpEc-parB P1
pMR YB	pMR10-*kan* ygfp-parB pMT1
pMR YB CB	pMR10-*kan* ygfp-parB pMT1 cfpEc-parB P1

Table displaying the name and associated genotype of the different strains which have been used in the results section of this master thesis. As described in the two lower tables, "P1" refers to *parS* P1 and "pMT1" refers to *parS* pMT1, while pMR CB, YB, and YB CB refer to pMR10-*kan cfpEc-parB* P1, *ygfp-parB* pMT1, and *ygfp-parB* pMT1 *cfpEc-parB* P1, respectively.

Figure 10

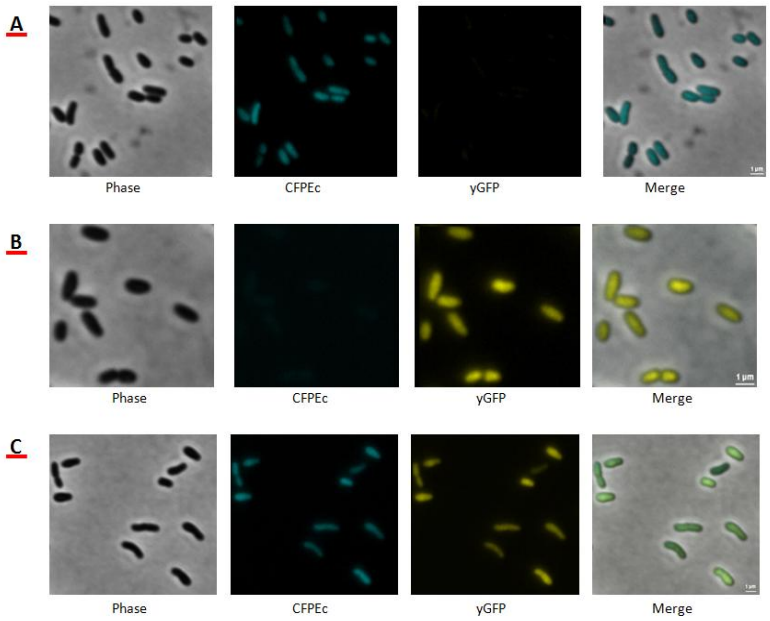

Phase contrast and fluorescence micrographs showing the expression of the differents XFP-ParB* used during this master thesis in non *parS**-labelled strains. A) CFPEC-ParB P1 in *B. abortus* pMR10-*kan cfpEc-parB* P1, B) yGFP-ParB pMT1 in *B. abortus* pMR10-*kan ygfp-parB* pMT1, C) both CFPEC-ParB P1 and yGFP-ParB pMT1 in *B. abortus* pMR10-*kan ygfp-parB* pMT1 *cfpEc-parB* P1. In each case, the signal is uniformly distributed in the bacterium, this absence of foci in the control strain (without *parS** sequence) being a prerequisite to start the localization of various chromosomal sites.

induce *parS** integration-mediated toxicity and/or disregulation, since head-to-head orientation suggests the absence of promoter regions.

Strains constructions

Due to the absence of modifications as compared to the work presented in June, the detailed strain construction section has been placed in annex (see annex number 1). In fact, only the last steps of the final *xfp-parB** carrying plasmid construction and the different PCR checks performed in order to confirm the insertion of *parS** in *B. abortus* were added. Instead, this section has been replaced by a recapitulative chart summarizing the different *B. abortus* strains used during this work as well as a brief description of their respective genotypes (see Table 1).

Control conditions

In order to validate the exploitability of the data generated with the *parS**/ParB* systems in *B. abortus* 544, several control conditions had to be tested prior to further investigations.

As stated in the introduction, each of the two exogenous P1 and pMT1 systems are functional analogs of *B. abortus* endogenous chromosome segregation mechanisms. Consequently, one can imagine that these exogenous systems could possibly interfere with *B. abortus* endogenous segregation systems, even though both ParB P1 and ParB pMT1 are specifically truncated in order to reduce such a probability (see "Introduction", fourth paragraph of the "Cell cycle blockade and its investigation" section). Therefore, we first had to make sure that no interference would be observed between endogenous *B. abortus* chromosomes segregation systems and the exogenous parS*/ParB* systems. To test this hypothesis, each of the three ParB* fusion-encoding plasmids (pMR10-*kan ygfp-parB* pMT1, pMR10-*kan cfpEc-parB* P1, and pMR10-*kan ygfp-parB* pMT1 *cfpEc-parB* P1) were separately placed in wild-type *B. abortus* 544 strain by mating from *E. coli* S17-1 strain (see "Material and methods"). Our observations matched the expected phenotype, where clones carrying the pMR10-*kan ygfp-parB* pMT1plasmid expressed a non-localized (i.e. diffused) yGFP signal (see figure 10.A), while clones carrying the pMR10-*kan cfpEc-parB* P1 plasmid expressed a non-localized CFPEc signal (see figure 10.B). Also, clones carrying the pMR10-*kan ygfp-parB* pMT1 *cfpEc-parB* P1 plasmid expressed both fusion proteins without displaying any foci, meaning that each fusion protein was produced but would not recognize any *B. abortus* endogenous sequences in the absence of *parS** sequences (see figure 10.C). Additionally, it should be noted that the simultaneous expression of both fusions did not modify the bacterium morphology, suggesting a satisfactory fusion tolerance in *Brucella*.

Second, we had to make sure that, (1) the *parS**/ParB* systems generate foci and not only diffuse signal in *B. abortus*, and (2) as in *E. coli* and *C. crescentus*, no interference would occur between the *parS* P1/ParB P1 system and the *parS* pMT1/ParB pMT1 system.

Figure 11

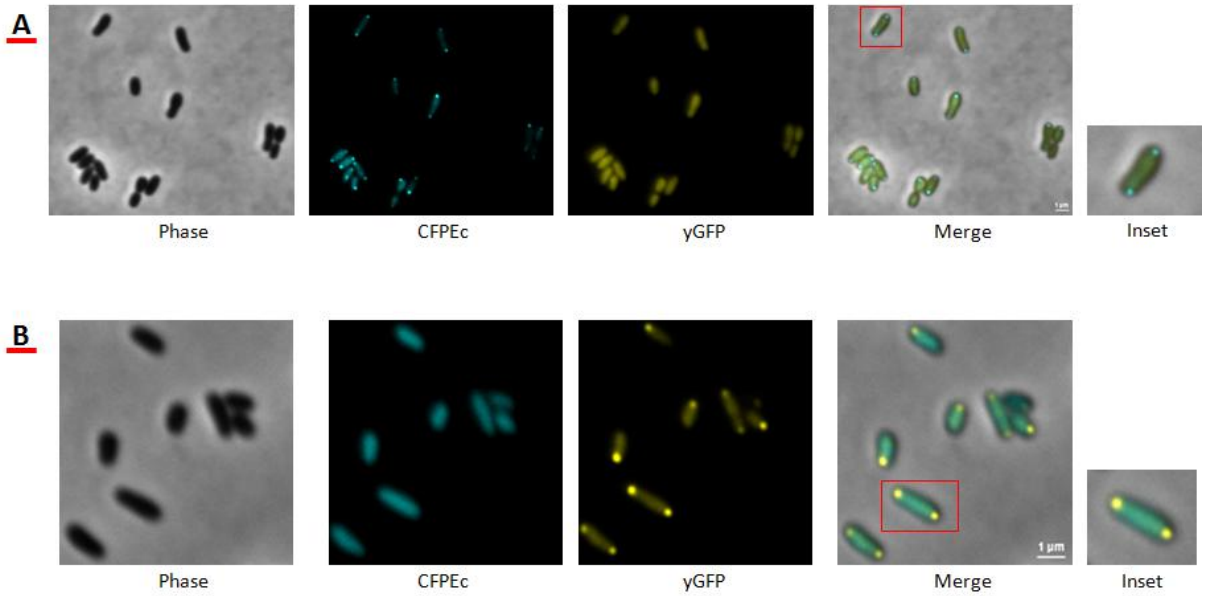

Phase contrast and fluorescence micrographs showing the expression of both XFP-ParB* fusion proteins with, in A) the specific localization of CFPEC-ParB P1 in *B. abortus Nori*I *parS* P1 pMR10-*kan ygfp-parB* pMT1 *cfpEc-parB* P1, and in B) the specific localization of yGFP-ParB pMT1 in *B. abortus Nori*I *parS* pMT1 pMR10-*kan ygfp-parB* pMT1 *cfpEc-parB* P1. The localization patterns suggest that CFPEC-ParB P1 and yGFP-ParB pMT1 are independent reporters, i.e. the focalized localization of one fusion does not generate a focalized localization of the other.

To test this hypothesis, two specific strains were generated. On the one hand, *B. abortus* 544 ***Nori*I *parS* P1**, and on the other hand, *B. abortus* 544 ***Nori*I *parS* pMT1**. Next, the pMR10-*kan* ygfp-parB pMT1 cfpEc-parB P1 plasmid was transferred in each of these two strains. Regarding *B. abortus* 544 *Nori*I *parS* **P1**, our observations matched the expected phenotype, where clones expressed both fusions, but only displayed specific signal localization for the CFPEc-ParB **P1** fusion, resulting in yellow-colored bacteria displaying either one or two blue foci, presumably depending on the replication state of chromosome I (see figure11.A). Regarding *B. abortus* 544 *Nori*I *parS* **pMT1**, our observations matched the expected phenotype, where clones expressed both fusions, but only displayed specific signal localization for the yGFP-ParB pMT1, resulting in blue-colored bacteria displaying either one or two yellow foci, probably depending on the replication state of chromosome II (see figure11.B).

As a general remark, it should be noted that all the conclusions presented in this work are mainly built upon qualitative analyses and therefore lack quantitative data. Such quantitative analyses are presently ongoing using the MicrobeTracker software (Sliusarenko *et al.* 2011) a recent software able to collect, analyze, and interrelate numerous parameters (for example, the number of foci and their intracellular localization correlated with the bacterium length) for a large number of bacteria using microscopy outputs (see "Discussion). This tool should hopefully allow us to numerically validate all the data detailed below, therefore strengthening our observations with statistical relevance.

Also, it should be noted that only cells displaying a wild type-like morphology were taken into account for the foci-associated phenotype analyses detailed below. Hence, cells displaying abnormal morphologies, which proportions varied in a strain-specific manner (see below), were discarded as they do not reflect a physiologically relevant state.

Single *parS** carrying strains

After validation of the P1 and pMT1 systems in *Brucella abortus*, we aimed at separately investigating the replication and segregation dynamics of the different chromosomal sites of interest that had been targeted. After a first round of *parS** insertion, four main strains were characterized in the *B. abortus* 544 background: ***Nori*I *parS* P1**, ***Nter*I *parS* P1**, ***Nori*II *parS* pMT1**, and ***Nter*II *parS* pMT1**, each of them possessing the pMR10-*kan ygfp parB* pMT1 *cfpEc parB* P1 plasmid. The fact of using the pMR10-*kan* plasmid with both fusion genes in strains possessing only one single *parS** sequence was used as a systematic control condition in order to discriminate actual foci from potential inclusion bodies. In fact, the overproduction of the fusion proteins could lead to the formation of aggregates displaying non-specific fluorescence, which could thus possibly interfere with the monitoring of *bona fide* foci. However, the fact of observing a focus of a single color while conserving a non-localized signal for the other fluorochrome tends to indicate the absence of inclusion bodies, and thus, validates the observed localized signal as an actual focus.

Figure 12

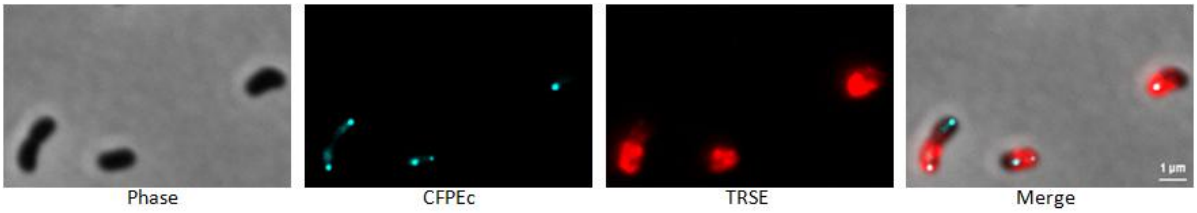

Phase contrast and fluorescence micrograph of *B. abortus Nori*I *parS* P1 pMR10-*kan ygfp-parB* pMT1 *cfpEc-parB* P1 showing the recurrent polar localization of the *Nori*I-associated CFPEC-ParB P1 focus/foci. The TRSE-mediated old pole staining (red) highlights the old pole localization of the *Nori*I locus in bacteria displaying a single *Nori*I-associated CFPEC-ParB P1 focus. For clarity reasons, the non-focalized yGFP signal is not shown here.

Figure 13

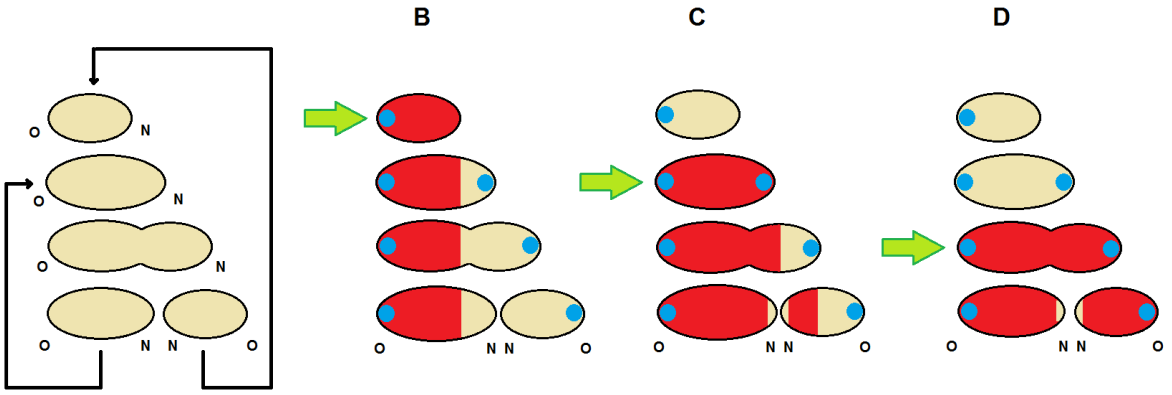

Schematic representation of TRSE-stained the *B. abortus Nori*I *parS* P1 strain highlighting the different labeling patterns observed depending on the cell cycle status of the bacterium (B, C, or D) when stained. We see, on the last row of column C, that the newly generated "small cell" displays a (somewhat counter-intuitive) new pole TRSE staining. (O: old pole, N: new pole, red: TRSE staining, blue dot: *Nori*I-associated focus/foci, green arrow: cell cycle status-specific TRSE labeling event).

Figure 14

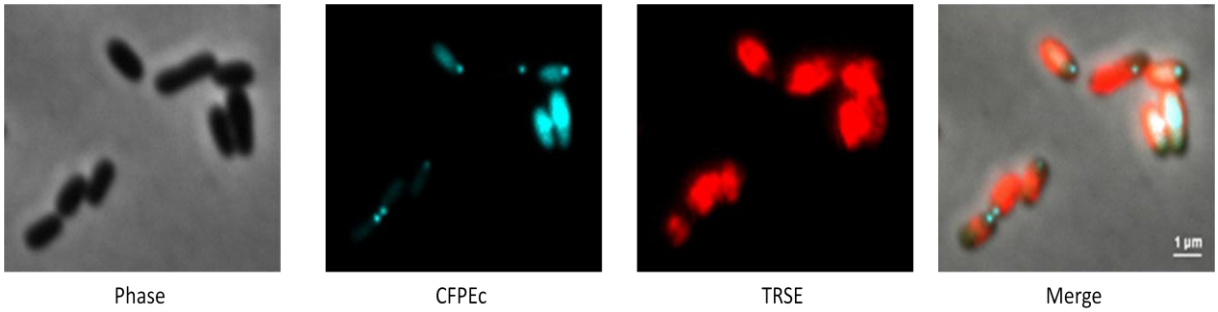

Phase contrast and fluorescence micrographs of *B. abortus Nter*I *parS* P1 pMR10-*kan ygfp-parB* pMT1 *cfpEc-parB* P1. The TRSE-mediated old pole staining (red) highlights the new pole localization of the *Nter*I locus in the shortest bacteria (typically about 1 µm), and its relocalization towards the midcell position in longer cells and predivisional cells. For clarity reasons, the non-focalized yGFP signal is not shown here.

Regarding *B. abortus* ***Nori*I *parS* P1**, we observed that the origin of replication of chromosome I displayed a reproducible localization pattern. In fact, when observing a sample of liquid culture harvested in the middle of its exponential phase (OD_{600} typically ranging between 0.4 and 0.6), it has been observed that the shortest cells (typically about 1 µm) only display a single polar focus, whereas in longer cells (typically 1,5 µm and more), a second focus is observed. In most cases, the second focus was predominantly located at the opposite cell pole, thus adopting a bipolar pattern (see figure12), even though in a few cells, this second focus has be found anywhere between the first focus and the opposite cell pole. Additionally, it has been observed that predivisional cells which have entered cytokinesis are characterized by a strictly bipolar pattern (see figure 12). Also, it should be noted that cells displaying other localization patterns (such as the absence of any focus or the presence of more than two foci) were either not observed, or observed in very low proportions.

Then, to assess the localization of the different foci in relation to the nature of the cell poles (growing or non-growing, i.e. new or old, respectively), we decided to perform TRSE labeling. TRSE (Texas Red Succinimidyl Ester) is a non-lethal dye composed of a succinimidyl group reacting with amines, coupled to the "Texas Red" fluorochrome. In our case, the TRSE molecules react with *B. abortus* surface (at least with the available lysines of the outer membrane proteins), resulting in the staining of the complete bacterial surface (Brown *et al.* 2012). Consequently, when bacteria are re-cultured for a short period of time after staining, the incorporation of newly synthesized cell wall material (thus unlabelled) allows us to identify the envelope growth zone by negative staining, thus enabling us to discriminate the growing pole (TRSE unlabeled) form the non-growing pole (TRSE labeled). After performing TRSE labeling (see "Material and methods"), we observed that, after cell division, the single CFPEc-ParB P1 polar focus was systematically located at the old cell pole (see figure 12).

It should be noted that some TRSE labeling artefact may be observed. In fact, when working on an unsynchronized population, TRSE labeling is applied on cells which are found in every cell cycle stages.Therefore, when cells are labeled while being in their cell cycle C phase, it is possible to generate artifactual daughter cells displaying a new pole TRSE labeling (see figure 13).

It should be noted that, according to these data, the origin of replication of chromosome I appears to follow a segregation pattern very similar to the distribution of mCherry-ParB as observed in both *C. crescentus* (Mohl & Gober, 1997) and in *B. abortus* (Deghelt *et al.* unpublished).

Regarding *B. abortus* 544 ***Nter*I *parS* P1**, we observed that the terminus region of chromosome I displays a reproducible segregation pattern. In fact, after harvesting a sample of liquid culture in its exponential phase and performing TRSE labeling, we have observed that the shortest cells only display one single polar focus located at the new cell pole. In longer cells however, we observed that the majority of cells display a single focus located at the midcell, while a few other cells display a focus located anywhere between a midcell and a polar position (see figure 14). Additionally, in predivisional cells, only one single focus is

Figure 15

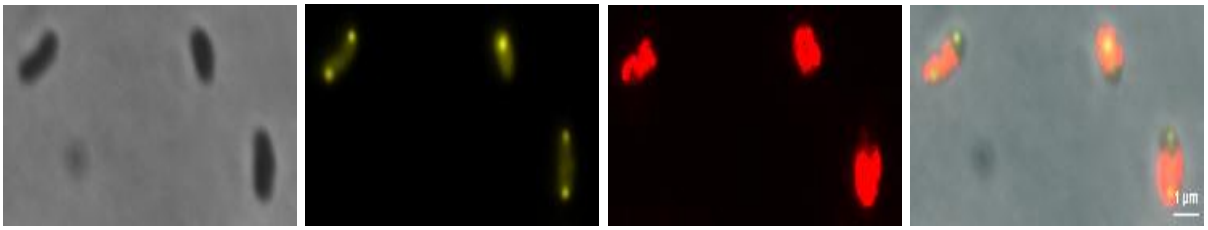

Phase contrast and fluorescence micrographs of *B. abortus Nori*II *parS* pMT1 pMR10-*kan ygfp-parB* pMT1 *cfpEc-parB* P1 showing the recurrent (near) polar localization of the *Nori*II-associated yGFP-ParB pMT1 focus/foci. The TRSE-mediated old pole staining (red) highlights the (near) old pole localization of the *Nori*II locus in bacteria displaying a single *Nori*II-associated yGFP-ParB pMT1 focus. For clarity reasons, the non-focalized CFPEc signal is not shown here.

Figure 16

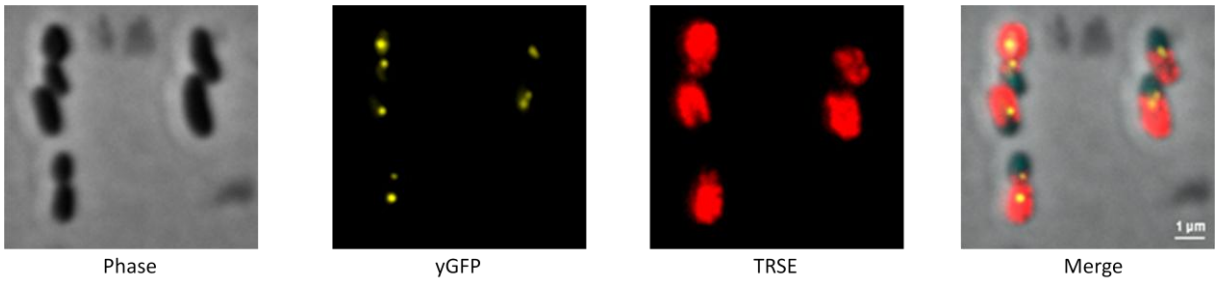

Phase contrast and fluorescence micrograph of *B. abortus Nter*II *parS* P1 pMR10-*kan ygfp-parB* pMT1 *cfpEc-parB* P1. The TRSE-mediated old pole staining (red) highlights the systematic (near) new pole localization of the *Nter*II locus in the shortest bacteria (typically about 1 µm), and its delocalization towards the midcell position and duplication in longer cells (typically about 1.5 µm). For clarity reasons, the non-focalized CFPEc signal is not shown here.

observed, even if cells have entered cytokinesis. However, when looking at cells displaying late constriction stage, two near foci could be distinguished. Also, it should be noted that, again, cells displaying other phenotypes (such as the absence of any focus or the presence of more than two foci) were either not observed, or observed in very low proportions.
To the best of our knowledge, these data represent the first localization of *B. abortus* chromosome I terminus region ever performed and, correlated with the localization patterns of the *Nori*I chromosomal site, these data suggest that *B. abortus* chromosome I displays an organized structure.

Regarding *B. abortus* 544 ***Nori*II *parS* pMT1**, we observed that the origin of replication of chromosome II displayed a reproducible segregation pattern. In fact, after harvesting a sample of liquid culture in its exponential phase and performing TRSE labeling, we have observed that the shortest cells only display one single focus **globally** located at the old cell pole. In fact, in the shortest cells, unlike the *ori*I, the position of the origin of replication of chromosome II was not always strictly anchored at the old cell pole, adopting a "globally polar" positioning. In longer cells, we observed the presence of a second focus predominantly located at the new cell pole, while in some cells, this focus could be found anywhere between the first focus and the new cell pole. It should be noted that, as for cells displaying a single focus, both foci displayed an either strictly polar or near polar localization, resulting in a globally bipolar pattern (see figure 15). Additionally, it has been observed that predivisional cells which have started constriction were characterized by the presence of a globally bipolar pattern, with each foci located at or near the future old cell poles. Also, it should be noted that cells displaying other phenotypes (such as the absence of any focus or the presence of more than two foci) were either not observed, or observed in extremely low proportions.
According to these data, the origin of replication of chromosome II appears to follow a globally polar segregation pattern similar to the distribution of RepB as observed in *B. abortus* with the YFP-RepB fusion protein (Deghelt *et al.* unpublished). However, our data do not perfectly match these previous observations, as a high proportion of the cells observed using our experimental settings display strictly polar foci. Therefore, foci localization analyses using the MicrobeTracker software (Sliusarenko *et al.* 2011) have to be performed (see "Discussion") to have a statistically valid interpretation of these data.

Regarding *B. abortus* 544 ***Nter*II *parS* pMT1**, we observed that the terminus region of chromosome II also displays a reproducible segregation pattern. In fact, after harvesting a sample of liquid culture in its exponential phase and performing TRSE labeling, we have observed that the shortest cells were characterized by the presence of only one single polar focus located either at or near the new cell pole. In longer cells however, we observed the presence of either one single midcell focus or two neighboring midcell foci (see figure 16). Also, it has been observed that predivisional cells which have entered cytokinesis were characterized by the presence of two foci localized close to the constriction site (see figure16). Again, it should be noted that cells displaying other phenotypes (such as the absence of

Figure 17

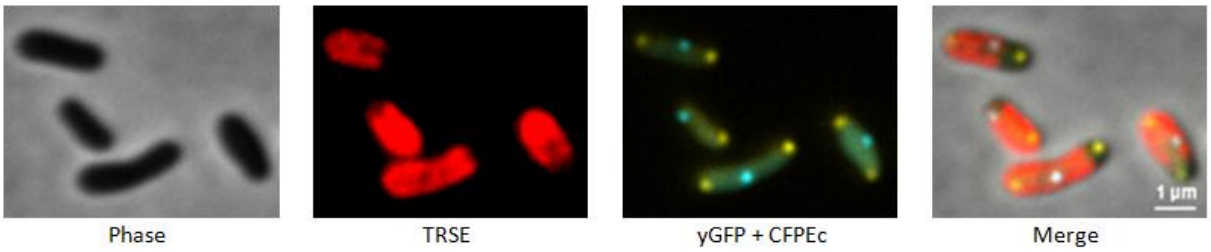

Phase contrast and fluorescence micrographs of *B. abortus Nori*I *parS* pMT1 *Nter*I *parS* P1 pMR10-*kan ygfp-parB* pMT1 *cfpEc-parB* P1. In the shortest bacteria (typically about 1 µm), the TRSE-mediated old pole staining (red) highlights the old pole and new pole localization of the *Nori*I and *Nter*I loci, respectively. In longer cells (typically about 1.5 µm or more) the *Nori*I-associated focus is duplicated and polarly localized while the single *Nter*I-associated focus is located at the midcell position. For clarity reasons, the CFPEc and yGFP signals are simultaneously displayed on a single image.

any focus or the presence of more than two foci) were either not observed, or observed in very low proportions.
To the best of our knowledge, these data represent the first localization of *B. abortus* chromosome II terminus region ever performed, also being the first localization of a *repABC* chromosome/megaplasmid *ter* region. When correlated with the localization patterns of the *Nori*II chromosomal site, these data suggest that *B. abortus* chromosome II also displays an organized structure. However, due to the apparent plasticity of its positioning patterns, *B. abortus* chromosome II appears to be subjected to a less strict positioning as compared to chromosome I for which localization patterns appear to be more robust.

Double *parS* * carrying strains

After observing and analyzing the localization patterns of each of the four chromosomal sites alone, we aimed at investigating *B. abortus* chromosome replication and segregation dynamics using strains possessing two *parS** sequences located at specific chromosomal sites (referred to as "double *parS**-carrying strains"). The fact of simultaneously monitoring the distribution of two distinct chromosomal sites, using strains displaying specific combinations of *parS**-labeled sites, allowed us to conduct two distinct strategies. On the one hand, we performed a "chromosome-based" approach, where we constructed two strains for which both the *ori* and the *ter* regions of a given chromosome were simultaneously *parS**-labeled, and on the other hand, we performed a "replication-based" approach, where we constructed two strains for which both *ori*s and, separately, both *ter*s were *parS**-labeled in order to analyze initiation and termination or replication, respectively (see "Objectives").

Regarding the "chromosome-based approach", two strains were constructed in the *B. abortus* 544 background: the chromosome **I**-specific strain ***Nori*I *parS* pMT1 *Nter*I *parS* P1**, and the chromosome **II**-specific strain ***Nori*II *parS* pMT1 *Nter*II *parS* P1**.

When culturing *B. abortus* ***Nori*I *parS* pMT1 *Nter*I *parS* P1** *in vitro*, we observed reproducible foci segregation patterns which were identical to those observed for *Nori*I and *Nter*I when analyzed separately (see "single *parS**-carrying strain"). In fact, after harvesting a sample of liquid culture in its exponential phase and performing TRSE labeling, we have observed that the shortest cells were characterized by the presence of a single *Nori*I-associated focus at the old cell pole and a single *Nter*I-associated focus at the new cell pole (see figure 17). In longer cells, a second *Nori*I-associated focus is present and predominantly localized at the opposite pole, while in some cells, it could be found anywhere between the initial polar focus and the new cell pole (see figure 17). Also, in these cells, the *Nter*I-associated focus remains unduplicated and found anywhere between the new cell pole and the midcell. In the longest cells and in cells which have started constriction however, both *Nori*I-associated foci are strictly located at the cell poles while the single *Nter*I-associated focus is located at the midcell position (see figure 17).
These data confirm the observations made for *Nori*I and *Nter*I as detailed in the "single *parS**-carrying strains" section, suggesting an ordered chromosomal structuring of *B. abortus*

Figure 18

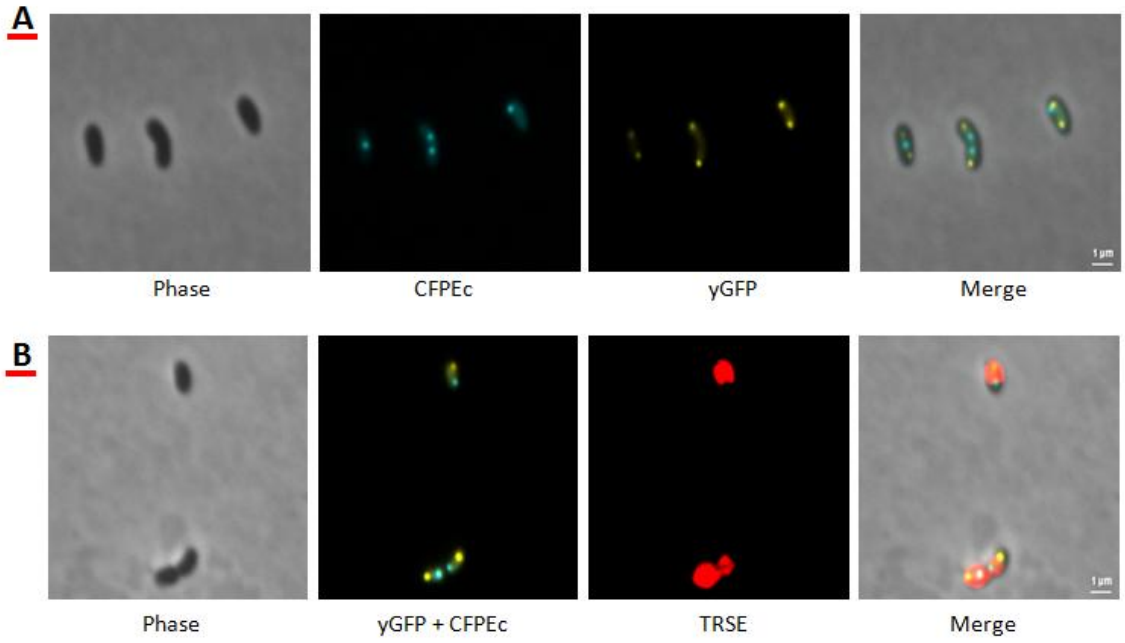

Phase contrast and fluorescence micrographs of *B. abortus Nori*II *parS* pMT1 *Nter*II *parS* P1 pMR10-*kan ygfp-parB* pMT1 *cfpEc-parB* P1 highlighting A) foci distribution patterns identical to those observed for the single *parS**-carrying strains when observed separately. B) In the shortest bacteria (typically about 1 µm), the TRSE-mediated old pole staining (red) highlights the (near) old pole and (near) new pole localization of the *Nori*II and *Nter*II loci, respectively. In longer cells (typically about 1.5 µm or more) both the *Nori*II-associated and the *Nter*II-associated foci are duplicated and localized either at or close to the old and the midcell position, respectively. For clarity reasons, the CFPEc and yGFP signals are simultaneously displayed on a single image.

chromosome I. Unfortunately, this reporter system does not allow us to monitor chromosome I replication termination due to absence of observable *Nter*I-associated focus duplication (see "Discussion").

When culturing *B. abortus* ***Nori*II *parS* pMT1 *Nter*II *parS* P1** *in vitro*, we observed reproducible foci segregation patterns which were identical to those observed for *Nori*II and *Nter*II when analyzed separately (see "single *parS**-carrying strain") (see figure 18.A). In fact, after harvesting a sample of liquid culture in its exponential phase and performing TRSE labeling, we have observed that the shortest cells were characterized by the presence of a single *Nori*II-associated focus, located either at or close to the old cell pole, and a single *Nter*II-associated focus located either at or near the new cell pole (see figure 18.B). In longer cells, a second *Nori*II-associated focus is present and predominantly localized at or close to the new pole, while in some cells, it may be found anywhere between the initial polar focus and the new cell pole. Also, in these cells, a single *Nter*II-associated focus is often found at the midcell while, in some cells, this focus is duplicated, resulting in two neighboring midcell foci (see figure 18.A). In the longest cells and in cells which have started constriction however, both the *Nori*II and the *Nter*II-associated foci have been duplicated and segregated in their respective future daughter cells, being localized either at or close to old cell poles and new cell poles, respectively (see figure 18.A/B).
These data confirm the observations made for *Nori*II and *Nter*II as detailed in the "single *parS**-carrying strain" section, suggesting an ordered chromosomal structuring of *B. abortus* chromosome II. Also, unlike chromosome I, this reporter system allows us to monitor both chromosome II replication initiation (characterized by the presence of two *Nori*II foci and a single *Nter*II focus) and replication termination (characterized by the presence of two *Nori*II foci and two *Nter*II foci). However, again, regarding *Nori*II, our data do not perfectly match previous observations of the YFP-RepB localization. In fact, a high proportion of the cells observed using our experimental settings displayed strictly polar *Nori*II-associated foci, as opposed to the systematic near-pole positioning observed with the YFP-RepB fusion protein (Deghelt *et al.* unpublished). However, again, foci localization analyses using the MicrobeTracker software (Sliusarenko *et al.* 2011) have to be performed in order to statistically address these interpretations (see "Discussion"). Additionally, it should be noted that, unlike the single *parS**-carrying strains, the double *parS**-carrying strains globally display more cells with aberrant morphology and absence of one or both fusion protein signal(s) (see "Discussion").

Regarding the "replication-based approach", two strains were constructed in the *B. abortus* 544 background: the **replication initiation**-specific strain ***Nori*I *parS* P1 *Nori*II *parS* pMT1**, and the **replication termination**-specific strain ***Nter*I *parS* P1 *Nter*II *parS* pMT1**.

Regarding *B. abortus* ***Nori*I *parS* P1 *Nori*II *parS* pMT1**, it should be noted that, as the other double *parS**-carrying strains, the double *Nori*I *Nori*II *Brucella* is subjected to several problems such as the presence of aberrant morphologies or the absence of one or both fusion proteins signal(s). However, this strain specifically displays these problems in a highly aggravated way. In fact, cells displaying an *a priori* decent phenotype, corresponding to the combination of *Nori*I and *Nori*II as in the "single *parS**-carrying strain" section, were only present at a very low frequency. Indeed, a high proportion of the observed cells displayed

Figure 19

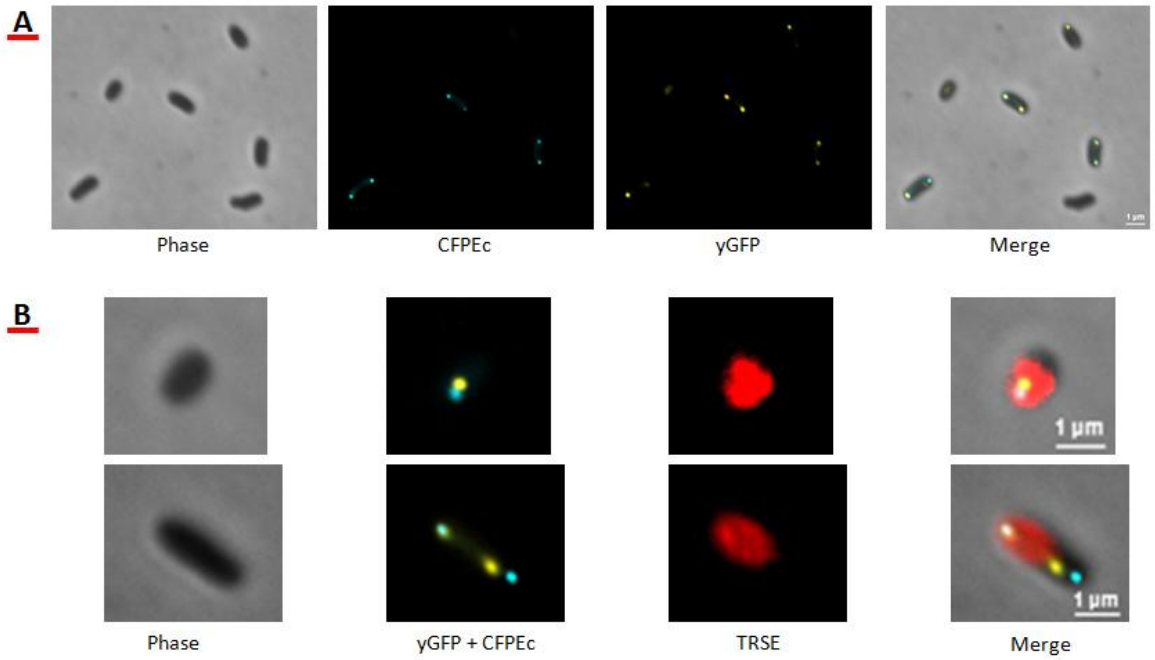

Phase contrast and fluorescence micrographs of *B. abortus Nori*I *parS* P1 *Nori*II *parS* pMT1 pMR10-*kan ygfp-parB* pMT1 *cfpEc-parB* P1 highlighting A) foci distribution patterns identical to those observed for the single *parS**-carrying strains when observed separately. Some bacteria do not display fluorescent foci, highlighting the problems of these strains as explained in the text. B) Due to the numerous morphological and phenotypical issues observed with this strain, two single cell observations are shown, displaying, on the upper row, a typically member of the shortest bacteria (about 1 µm), and, on the lower row, a typically member of the longer bacteria (about 1.5 µm or more). The TRSE-mediated old pole staining (red) highlights the old pole and near old pole localization of the *Nori*I and *Nori*II loci, respectively. For clarity reasons, the CFPEc and yGFP signals are simultaneously displayed on a single image.

Figure 20

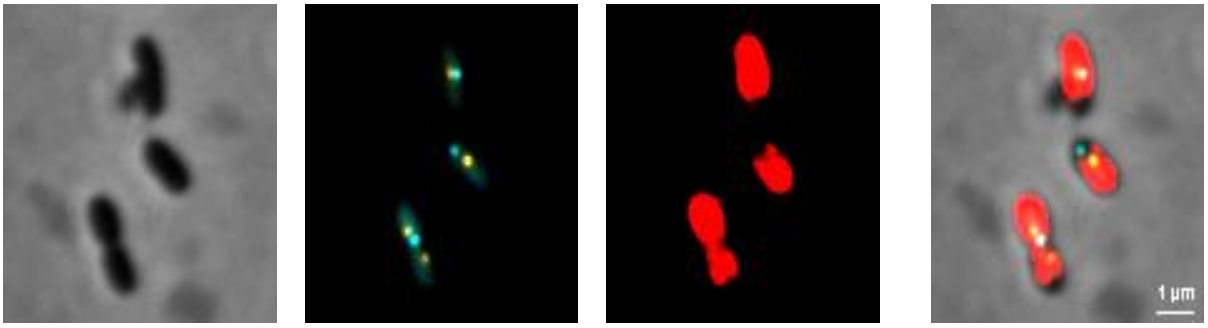

Phase contrast and fluorescence micrographs of *B. abortus Nter*I *parS* P1 *Nter*II *parS* pMT1 pMR10-*kan ygfp-parB* pMT1 *cfpEc-parB* P1 highlighting foci distribution patterns identical to those observed for the single *parS**-carrying strains when observed separately. In the shortest bacteria (typically about 1 µm), the TRSE-mediated old pole staining (red) highlights the new pole and (near) new pole localization of the *Nter*I and *Nter*II loci, respectively. In longer cells (typically about 1.5 µm or more) both the *Nter*I and the *Nter*II loci are found at and close to the midcell position, respectively, where only the *Nter*II-associated focus is found to be duplicated. For clarity reasons, the CFPEc and yGFP signals are simultaneously displayed on a single image.

only a single focalized signal (either the CFPEc-ParB P1 signal or the yGFP-ParB pMT1 signal), with no obvious selection bias, while the other fusion protein signal was either absent or present but unlocalized (see "Discussion"). Nonetheless, when specifically analyzing cells displaying wild type-morphology while expressing both fusion proteins, we observed reproducible foci segregation patterns which were identical to those observed for *Nori*I and *Nori*II when analyzed separately (see "single *parS**-carrying strain") (see figure19.A). In fact, after harvesting a sample of liquid culture in its exponential phase and performing TRSE labeling, we have observed that the shortest cells were characterized by the partial colocalization of a single *Nori*I-associated focus located at the old cell pole and a single *Nori*II-associated focus located either at the old cell pole (see figure19.B). In longer cells, both the *Nori*I and the *Nori*II chromosomal sites are duplicated and segregated, resulting in a bipolar colocalization of the *Nori*I-associated foci and the *Nori*II-associated foci (see figure19.B).

Regarding *B. abortus* ***Nter*I *parS* P1 *Nter*II *parS* pMT1,** it should firstly be noted that, as hinted in the "single *parS**-carrying strain" section, this strain only allows us to monitor chromosome replication termination of chromosome II, as the *Nter*I-associated focus is not visibly duplicated. Therefore, this strain failed at highlighting an eventual termination-based chromosome replication synchronization in *B. abortus*. Nevertheless, such a tool was found to be helpful in order to answer other biological questions (see "Discussion").
Nonetheless, when culturing *B. abortus Nter*I *parS* P1 *Nter*II *parS* pMT1 *in vitro*, we observed reproducible foci segregation patterns which were identical to those observed for *Nter*I and *Nter*II when analyzed separately (see "single *parS**-carrying strain"). In fact, after harvesting a sample of liquid culture in its exponential phase and performing TRSE labeling, we have observed that the shortest cells were characterized by the presence of a single *Nter*I-associated focus, located at the new pole, and a single *Nter*II-associated focus, located at or near the new cell pole (see figure 20). In longer cells, the *Nter*II-associated focus is predominantly localized at a quarter cell to midcell position and, in a few cells, this focus is duplicated, resulting in two neighboring foci located at the midcell. Conversely, the *Nter*I-associated focus is found anywhere between the new pole and a near-midcell position while remaining unduplicated (see figure 20). In the longest cells and in cells which have entered cytokinesis however, both the *Nter*II foci are clearly duplicated and located on either sides of the constriction site near the future daughter cell new poles, while the *Nter*I-associated focus is systematically located at the midcell but remains predominantly unduplicated (see figure 20).
These data represent the first simultaneous localization of *B. abortus* chromosomes termini regions. Additionally, these observations confirm the data obtained for *Nter*I and *Nter*II as detailed in the "single *parS**-carrying strain" section. Again, it should be noted that, unlike the single *parS**-carrying strains, the double *parS**-carrying strains globally display more cells with aberrant morphologies and absence of one or both fusion proteins signal(s) (see "Discussion").

Additionally, we tried to assess which of the *ori*I or *dnaA* locus was the actual origin of replication of chromosome I. To do so, we constructed a strain with a specific combination

Figure 21

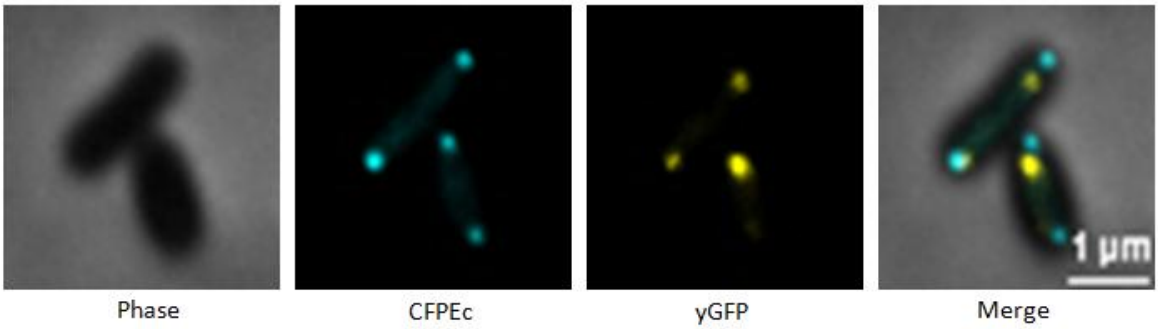

Phase contrast and fluorescence micrographs of *B. abortus Nori*I *parS* P1 *NdnaA parS* pMT1 pMR10-*kan ygfp-parB* pMT1 *cfpEc-parB* P1 highlighting the duplication of the *Nori*I focus prior to the *NdnaA* locus, thus designating the *Nori*I locus as the likeliest *B. abortus* chromosome I origin of replication, if confirmed by further quantitative analysis.

of *parS** sequences located at chromosomal sites located near these two loci: *B. abortus* 544 ***Nori*I *parS* P1 *NdnaA parS* pMT1**. For every stages of the cell cycle, we mainly observed a neighboring distribution of *Nori*I-associated foci and *NdnaA*–associated foci, where *Nori*I-associated foci were found to be distributed as detailed above, while the *NdnaA*–associated foci systematically displayed a more internal localization. However, a few cells clearly displayed a duplicated *Nori*I-associated focus while conserving a single *NdnaA*–associated foci, whereas the opposite situation was never encountered (see figure 21). Such data highlight the fact that the *Nori*I region is duplicated prior to the *NdnaA* as hinted by our *in silico* analyses, thus suggesting that the *ori*I locus, as opposed to the previously predicted *dnaA* locus, is the actual origin of replication of *B. abortus* chromosome I.

FACS strains analysis

After observing and mostly qualitatively analyzing the foci localization patterns of the different single and double *parS**-carrying strains detailed above, we decided to analyze the respective abundance of the 1n (or B phase), S (or C phase) and 2n (or D phase) sub-populations for each strain, and to compare these values with referential values. In fact, we know, based on our observations, that the genomic insertion of several *parS** sequences along with the expression of XFP-ParB* fusion proteins in *B. abortus* somehow generates perturbations, as observed morphologically. Consequently, in order to try to quantify this physiological impact, we decided to perform FACS analyses correlating the DNA content (x-axis), monitored by the fluorescence intensity displayed by permeabilized cells incubated with Sytox Green (see "Material and methods"), with the number of counted bacterial cells (y axis), thus obtaining strain-specific profiles. Once obtained, these profiles were separately compared to a reference culture for the percentage of cells found in both 1n (or B phase) and S + 2n (both C and D phases) (see figure 22). We chose to group the S and 2n categories because they represent the bacteria that have duplicated their replication origins, by contrast to the 1n cells which did not replicate their replication origins. It should be noted that, due to the difficulty to perform statistical tests on such results, consequent to the absence of replicated cultures, an arbitrary limit has been set to 5 % for the changes that we be considered for the comparison between strains.

First, we analyzed a wild type *B. abortus* strain in order to standardize the FACS detection parameters (see "Material and methods"). Then, after setting a standard gate (typically 200 units in the fluorescence channel of and above), we compared this first profile to the profile of *B. abortus* pMR10-*kan ygfp-parB* pMT1 *cfpEc-parB* P1 (see figure 22.A). With this comparison, we observed that the respective sub-populations proportions were not significantly different based on our criteria (see figure 22, lower right chart). Consequently, we decided to use *B. abortus* pMR10-*kan ygfp-parB* pMT1 *cfpEc-parB* P1 (referred to as "wt pMR YBCB" or, in this case strain "number 2") as the reference strain, considering the fact

Figure 22

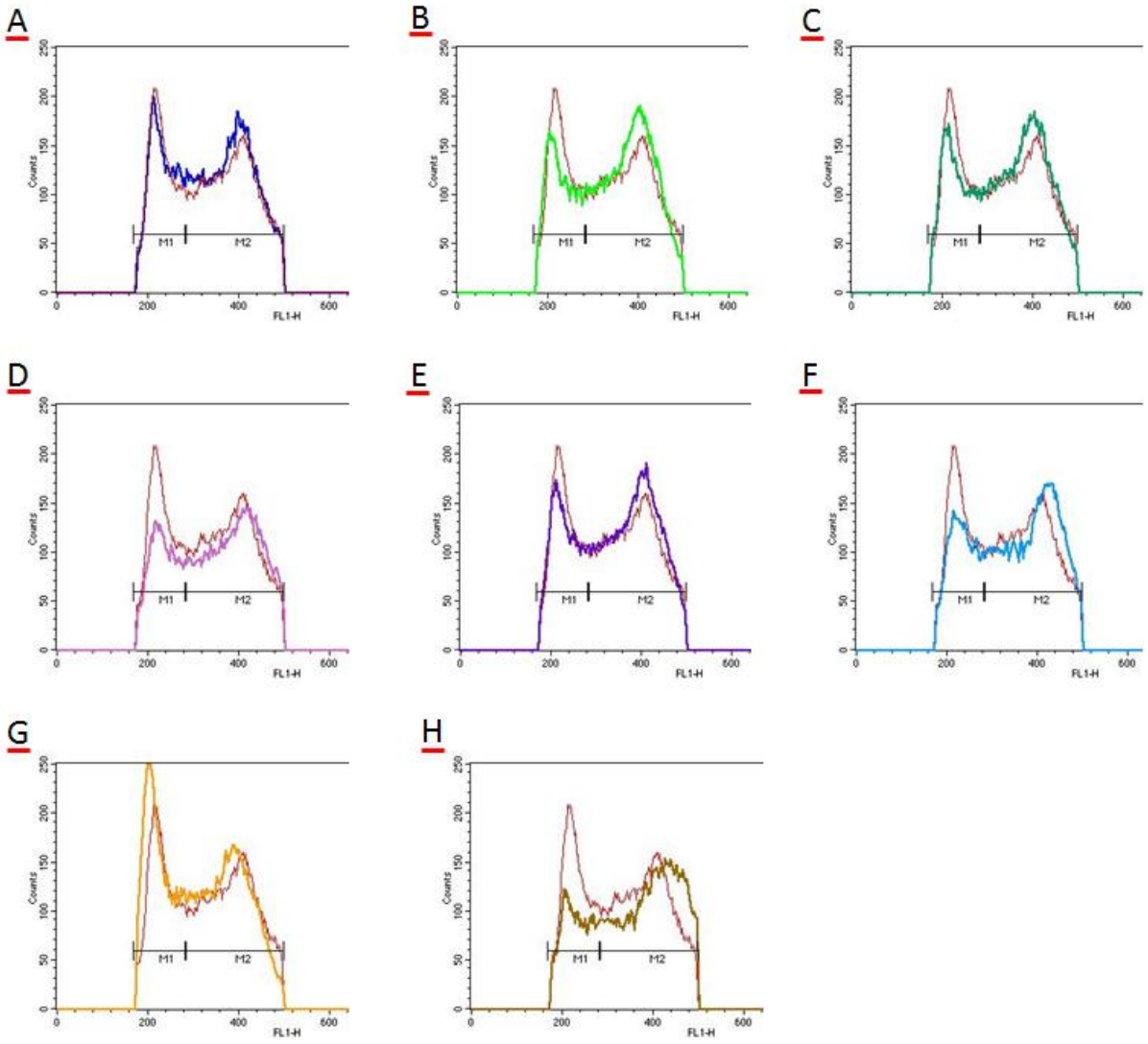

FACS profile	comparison
A	2 vs. 1
B	2 vs. 3
C	2 vs. 4
D	2 vs. 5
E	2 vs. 6
F	2 vs. 7
G	2 vs. 8
H	2 vs. 9

number	strains (B. abortus 544)	counts	gated counts	1n %	S + 2n %	1n - n°2	(S + 2n) - n°2
1	wt	84025	38051	34,4	65,6	-2,50	2,50
2	wt pMR YBCB	77930	36388	36,9	63,1	0,00	0,00
3	*Nor*I *parS* P1 pMR YBCB	262466	37069	32,0	68,0	-4,90	4,90
4	*Nter*I *parS* P1 pMR YBCB	109560	37116	32,5	67,5	-4,40	4,40
5	*Nor*II *parS* pMT1 pMR YBCB	69235	31918	30,9	69,1	-6,00	6,00
6	*Nter*II *parS* pMT1 pMR YBCB	102244	37528	32,6	67,4	-4,30	4,30
7	*Nor*I *parS p*MT1 *Nter*I *parS* P1 pMR YBCB	98999	35195	31,0	69,0	-5,90	5,90
8	*Nor*II *parS* pMT1 *Nter*II *parS* P1 pMR YBCB	163639	39768	41,5	58,5	4,60	-4,60
9	*Nter*I *parS* P1 *Nter*II *parS* pMT1 pMR YBCB	116729	33026	28,0	72,0	-8,90	8,90

FACS profiles displaying the fluorescence intensity (x axis) over the number of bacteria (y axis) of different *B. abortus* strains compared to the reference profile of *B. abortus* pMR10-*kan ygfp-parB* pMT1 *cfpEc-parB* P1 or strain n°2 (referred to as "wt pMR YBCB"). Each number corresponds to a specific strain (see table on the right), and each graph compares the profile of one of these strains to the reference strain n°2 profile (see table on the left). For every graph, the reference "wt pMR YBCB" profile is represented by a thin purple curve. In the table on the right, the percentage of 1n and S + 2n cells has been calculated for each strain (see columns "1n %" and "S + 2n %", respectively) and subtracted from the values obtained for the reference "wt pMR YBCB" strain n°2 (see column "1n – n°2" and "(S + 2n) – n°2").

that its genotype is more similar to the genotypes of the other tested strains as compared to the wild-type strain. The general pattern of the FACS analysis of these two strains is the presence of two peaks (one at 200-240 units and the other around 400 units in the FL1-H channel), of similar size. The profile is also characterized by a strong decrease of events with FL1-H intensities above 400 units, which could be interpreted as the absence (or the low frequence) of polyploïd cells (>2n genome content).

Then, by comparing our different strains with the "wt pMR YBCB" strain (see figure 22.B through H), several conclusions could be drawn. First, we saw that, for every strain, the changes in sub-populations proportions were around 5 %, being thus apparently slightly different from the reference strain as based on our criteria, but also always lower than 10 %. For all strains analyzed here, the general wild type-like pattern was conserved, except for the strain carrying a *parS** sequence at both *Nter* regions, in which some cells with an apparent genome content above 2n seem to be detectable. For the other strains analyzed here, it seems that the FACS analysis reveals only slight variations as compared to the control strain, suggesting that the majority of the bacteria examined in the previous section are similar to the wild type strain.
It should be noted that the *Nori*I *Nori*II strain was not analyzed considering the fact that this strain displayed major morphological and phenotypical problems (see "Double *parS** carrying strains" section), thus only permiting reduced qualitative analyses.

Discussion

Figure 23

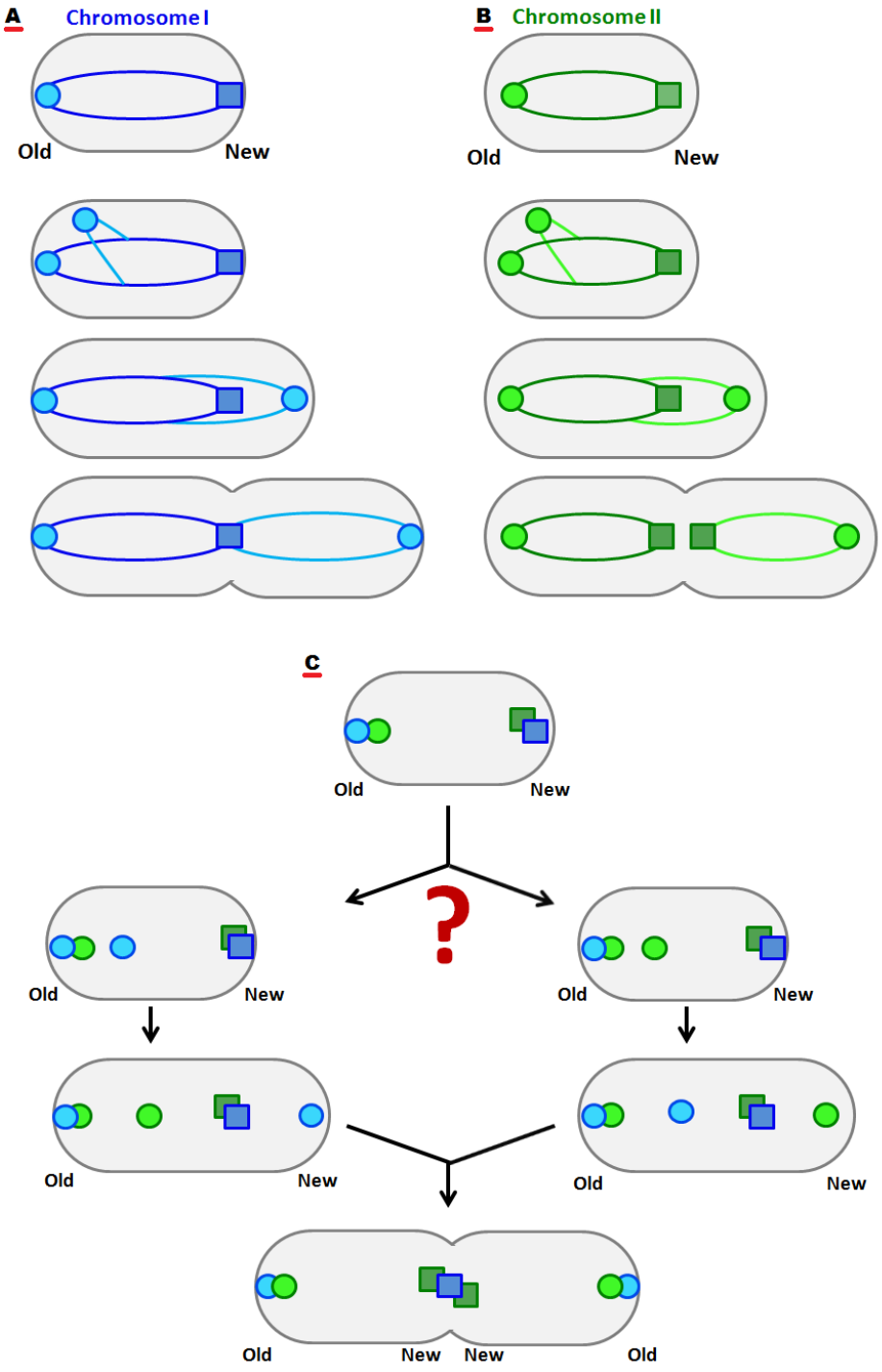

Hypothetical model of the replication and segregation of *B. abortus* chromosomes when cultured *in vitro*, constructed based on the qualitative data gathered during this master thesis (circles: *oris*, square: *ter*s, blue: chromosome I, green: chromosome II). A) Chromosome I replication and segregation patterns alone. B) Chromosome II replication and segregation patterns alone. C) Merging of the two chromosome profiles. The split sections represent two hypothetical scenarios of non initiation-synchronized chromosome replication, where, on the left arm, chromosome I replication is initiated prior to chromosome II, and on the right arm, chromosome II replication is initiated prior to chromosome I.

Discussion

In the light of the results detailed above, we have been able to show that the two chromosomes of *Brucella abortus* display specific and reproducible replication and segregation patterns. In fact, based on the monitoring of different and specifically labeled chromosomal sites, we can summarize the obtained data by the creation of a replication and segregation model of *B. abortus* chromosomes when cultured *in vitro* (see figure 23).
As a general remark, it should be noted that, as stated at the beginning of the "Results" section, all the conclusions presented in this work are mainly built upon qualitative analyses and therefore lack quantitative analysis. In fact, our model has only been built based on our observations and will thus require substantial experimental and quantitative data in order to be rigorously validated. It should be noted that such quantitative analyses will be conducted soon using the MicrobeTracker software (see "Results", last paragraph of the "control conditions" section) as well as extensive FACS analyses, for strains cultured in different culture media. With these analyses, we hope to be able to numerically validate the observations detailed below, by providing a statistical relevance.

A first observation is that the **origins** of replication of both chromosomes systematically display a globally polar localization (see figures 12, 15, and 19). In fact, based on our observations, we showed that short cells (presumably resulting from a recent cell division) are characterized by the presence of both *ori* regions located at the **old cell pole**. It should be noted that, even though sharing a globally polar localization, the two *ori*s display positioning difference. In fact, we observed that *ori*I is characterized by a strictly pole-anchored profile, whereas the positioning of *ori*II alternates between the old pole and midcell. Then, as the cell grows, an additional focus appears for each fusion, reflecting the initiation of chromosome replication. This additional focus is predominantly found at the new cell pole, resulting in a bipolar positioning pattern. This pattern seems to be kept until the end of cell constriction, resulting –after division– in two daughter cells displaying a single origin of replication for each chromosome located at their respective old poles.
Also, to the best of our knowledge, this work presents the first attempt of intrabacterial localization of the **termini** regions of *B. abortus* chromosomes (see figure figures 14, 16 and20). First of all, it should be noted that both termini displayed specific and reproducible segregation patterns, very different from those detected for the origins, suggesting that the position of the *parS* sequence on the chromosome does not systematically yield the localization pattern observed for the origins. Based on our observations, we showed that short cells (presumably resulting from a recent cell division) are characterized by the presence of both *ter* regions at the **new cell pole**. However, as observed with the *ori* regions, these patterns clearly highlighted chromosome-specific differences. Indeed, we observed that, even though sharing a globally polar localization, *ter*I is characterized by a rather pole-anchored profile, whereas *ter*II alternates between a polar and a near-pole positioning. Then, in larger cells, the *ter*II region appears to be quickly relocated at the midcell, as compared to the *ter*I

region which is less often visible at midcell in smaller cells. Eventually, both *ter* regions reach the midcell where they remain until cell division. Interestingly, only the *ter*II-associated focus has been observed as duplicated, whereas the presence of two *ter*I-associated foci has not been observed. This suggests that *ter*I replication and segregation is not observable in the conditions used here, and it is possible that *ter*I regions are duplicated but not segregated in the constricting cells for example (see below).

Based on these findings, we are able to propose that, firstly, the two *B. abortus* chromosomes possess a reproducible orientation inside the bacterium, where each *ori* is located at the old pole and each *ter* is located at the new pole. In fact, both chromosomes seem to display a *Caulobacter*-like "longitudinal" orientation, spanning from the old pole to the new pole (Toro & Shapiro, 2010), as opposed to the "transverse" *E. coli* model (Nielsen *et al.* 2006). Further investigation of this aspect of structural organization inside the bacterium would require the analysis of more strains, with *parS** sites inserted at several regions along the chromosomes.

Secondly, even though sharing structural orientation, the two *B. abortus* chromosomes also display specific differences regarding their replication/segregation dynamics. In fact, we observed that chromosome I *ori* and *ter* regions display highly robust localization patterns (detailed above), whereas chromosome II *ori* and *ter* regions display more variable localization profiles, portraying plausible evidence of an aggravated "structural breathing". Such differences could be an indication of the likely diverging evolutionary origin of these two chromosomes. In fact, our observations, correlated with previous work conducted in our lab (Deghelt *et al.* unpublished), seem to indicate that *B. abortus* chromosome I behaves as a "classical" bacterial chromosome, as exemplified in *C. crescentus*, while *B. abortus* chromosome II appears to behave as a more mobile element. This idea gets even stronger when considering the fact that chromosome I segregation system is highly similar to the *C. crescentus parABS* chromosomal segregation system, whereas chromosome II possesses typically plasmidic *repABC* replicon, and that no pole-anchoring mechanism has been discovered for this chromosome so far. Taken together, these facts support the likely hypothesis suggesting that *B. abortus* chromosome II is an actual essential genes-carrying megaplasmid that would have evolved from an ancestral plasmid, at least for its replication control system. Following this idea, we could thus hypothesize that the rather mobile nature of chromosome II, as compared to a systematically pole-anchored *bona fide* bacterial chromosome, could constitute some kind of a "legacy" inherited from its plasmidic ancestor.

Another objective of this work was to assess which of the *ori*I locus or the *dnaA* locus was the actual origin of replication of *B. abortus* chromosome I by constructing a strain where two chromosomal insertion sites neighboring these two loci of interest (*Nori*I and *NdnaA*) were specifically *parS**-labeled (see figure 21). With this strain, we observed that most cells displayed a similar phenotype where the *Nori*I-associated focus/foci displayed localization patterns identical to those described above, whereas the *NdnaA* associated focus/foci were found close to the *Nori*I-associated focus/foci while displaying a more "internal" localization

pattern. However, in some of the shortest cells, we observed a clearly duplicated *Nori*I-associated focus while conserving a single *NdnaA* associated focus. These data suggest that the *Nori*I locus is replicated and segregated prior to the *NdnaA* locus, at least in these cells, thus suggesting that the *ori*I locus, as opposed to the previously predicted *dnaA* locus (Chain *et al.* 2005), is the actual origin of replication of *B. abortus* chromosome I.

Additionally, another objective was to test a possible replication synchronization of *B. abortus* chromosomes. Unfortunately, our reporter systems failed at highlighting an either initiation-based or termination-based synchronization of *B. abortus* chromosomes replication, as detailed below.

On the one hand, the strain used to investigate a possible initiation-based synchronization of *B. abortus* chromosomes replication (*B. abortus* 544 *Nori*I *parS* P1 *Nori*II *parS* pMT1) only displayed a few cells able to express and localize both fusion proteins while conserving a wild-type morphology (see figures 12, 15, and19). In fact, most cells displaying a wild-type morphology expressed a functional version of only one of the two fusion proteins (with no striking preference), the other fusion being either unexpressed or expressed but unable to form a focus. Additionally, the remaining cells where characterized by aberrant morphologies and/or the absence of any expected fluorescence signal. A reason to observe such phenotypes is probably that the simultaneous expression of these two functional fusion proteins is toxic when two *parS** sequences are integrated in *B. abortus* chromosomes. This hypothesis is supported by the fact that, on average, the single *parS**-carrying strains display less cells with aberrant morphology/phenotype than the double *parS**-carrying strains. However, this reason alone does not unravel the entire problem since several double *parS**-carrying strains display less aberrant cells. In fact, as mentioned above, the morphology of *B. abortus* 544 *Nori*I *parS* P1 *NdnaA parS* pMT1 is comparable to the wild type strain while expressing and localizing both fusion proteins, resulting in a viable and physiologically valid phenotype displaying significant colocalization of both fusion proteins-associated foci. Consequently, the likeliest reason to justify *B. abortus Nori*I *parS* P1 *Nori*II *parS* pMT1 phenotypes could be that the toxicity of the binding of XFP-ParB* is locus-specific. This hypothesis is supported by the fact that it has been observed in plasmid P1 (know to be the genome of bacteriophage P1 in its lysogenic phase) that genes surrounding the centromere-like *parS* site were silenced due to the oligomerization and spreading of ParB onto DNA (Rodionov *et al.* 1999). We can thus hypothesize that the *cis* spreading of XFP-ParB* could likely impair the proper expression of neighboring genes, resulting in an altered function which could possibly lead to pleitropic phenotypes, including morphological alterations as described above. Therefore, one could imagine that, in this bacterial population, random mutation either resulting in the transcriptional inhibition or in the loss of function of one or both XFP-ParB* fusion proteins could have been greatly favorable on a Darwinian perspective, thus resulting in bulk positive. Interestingly, the phenotypic alterations of the strain with a *parS** inserted near both *ori*s are much more pronounced compared to those observed in strains displaying a single *parS**-inserted *ori*. In a sense, a "synthetic" phenotype is generated by these two simultaneous *parS** insertions, their effect being more synergic than additional, thus indicating a potential genetic interaction between the two mutated sites.

However, it should be noted that this genetic interaction could be very indirect and it would therefore be difficult to propose a mechanism explaining such synthetic phenotype.

On the other hand, the strain used to investigate a possible termination-based synchronization of *B. abortus* chromosomes replication (*B. abortus* 544 *Nter*I *parS* P1 *Nter*II *parS* pMT1) could not be used for this purpose since, as hinted in the "single *parS** carrying strains" section, the *Nter*I-associated focus never displayed any duplication. In fact, when observing predivisionnal cells or cells which have entered cytokinesis, we observed that, as opposed to *Nter*II-associated focus (which is clearly duplicated), the *Nter*I-associated focus remains at the midcell position until late constriction (see figure 20). However, our observation techniques are not precise enough to be able to distinguish a cell undergoing late cytokinesis from two newly separated daughter cells. Therefore, we never observed a duplicated *Nter*I region. Consequently, because only the replication termination of chromosome II can be faithfully monitored, we have been unable to test the possible termination-based synchronization of *B. abortus* chromosomes replication using our current experimental settings. However, this strain was found to be helpful regarding other biological questions. In fact, this strain helped us to show that, as opposed to the *Nori*I *Nori*II strain, double *parS** carrying strains could mostly display wild type-like morphologies (see above). Also, this strain showed that both termini regions simultaneously displayed specific localization patterns, thus implying the existence of chromosome-specific intrabacterial organization possibly suggesting a diverging evolutionary origin (see above).

Also, it should be noted that the absence of detectable *Nter*I-associated focus duplication cannot be straightforwardly linked to an absence of replication. Following this idea, one can imagine that the *ter*I locus could be replicated but not segregated until late constrictional stage, thus displaying a phenotype identical to the one described above (see figure 20).

Another objective was to either validate or refute previous work regarding chromosome replication initiation and localization by intracellularly localizing a *parS**-labeled *Nori*I site in a *B. abortus* 544 *mcherry-parB* strain, and, separately, by localizing a *parS**-labeled *Nori*II site in a *B. abortus* 544 *yfp-repB* strain. However, the construction of these two strains is still ongoing. Nevertheless, we have observed that, when comparing the localization patterns of mCherry-ParB with *Nori*I and YFP-RepB with *Nori*II, we obtain highly similar data. In fact, regarding the *ori*I, we observed that both the *Nori*I-associated focus/foci and the mCherry-ParB focus/foci display robust polar localization patterns, and that, in the same manner, we see that both YFP-RepB focus/foci and the *Nori*II-associated focus/foci display similar near-pole positioning patterns when considering the *ori*II. Consequently, it appears that, when taken separately, these different polar markers display highly similar profiles. Therefore, it is tempting to speculate that these tendencies could reflect a likely colocalization of these different *ori*s markers. Such results would allow us to indicate that mCherry-ParB and YFP-RepB could be reliable markers of the localization of the origin of replication of *B. abortus* chromosome I and II respectively, hence validating results yielded by experiments in which they have been used accordingly (Deghelt *et al.* unpublished). Nonetheless, these preliminary observations still have to be clearly validated through extensive observations of both a *B. abortus* 544 *mcherry-parB* strain carrying a a

*parS**-labeled *Nori*I site, and, separately, a *B. abortus* 544 *yfp-repB* strain carrying a *parS**-labeled *Nori*II site (see "Objectives").

As stated in the "Objectives" section, one of the main goal of this work was to test the cell cycle blockade hypothesis believed to characterize bacteria displaying the PdhS-/IfoP+ phenotype during the first hours of *B. abortus* infection cycle. For this matter, we mainly planned on using the *B. abortus* strain in which both *Nori* regions were specifically *parS**-labeled. However, due to the problems of such a strain, largely specified above, such an infection was found to be impossible. We thus propose to use the two single *parS**-carrying strains, in order to investigate the presence or absence of chromosome replication. The use of these strains would allow us to look for any chromosome replication initiation event in the early time post-infection. Also, we planned on using strains carrying *parS**-labeled *Nter* regions as a control, where the duplication of these regions could indicate an actual termination of chromosome replication. It should be noted that the findings regarding the absence of detectable *Nter*I duplication were brought to light afterward.
Unfortunately, due to repeated technical problems relative to HeLa cells culture, no infection could eventually been performed during this master thesis, consequently leaving us virtually standing one infection away from obtaining *in infectio* data regarding chromosome replication.

Finally, the *B. abortus* cell cycle has been characterized by several cell types (PdhS+/IfoP+, PdhS+/IfoP-, and PdhS-/IfoP+) (see "Introduction-Functional asymmetry in infection" section). However, this model does not take into account the initiation of chromosome replication. In the same context, the reporter systems generated during this master thesis currently lack the ability to faithfully discriminate the different *B. abortus* cell types, i.e. bacteria displaying the PdhS-/IfoP+ phenotype, the only discrimination presently being their ability to carry out infection. Following this idea, it would be interesting to evaluate the proportion of PdhS- bacteria that have duplicated and segregated their *ori*I and/or *ori*II loci in order to gain a better resolution of the different cell types encountered by *B. abortus* during its cell cycle. Consequently, we decided to solve these two problems by constructing strains simultaneously possessing our current reporter systems and the *pdhS-mcherry* fusion gene. Additionally, other perspectives could include the fact of adding a reliable polar marker such as the *popZ-mcherry* fusion gene. Such strains are presently under construction.
Also, another major perspective would be to perform time lapse imaging on most of the strains described above. In fact, such analyses should allow us to obtain valuable temporal information, thus enabling us to clearly define chromosomal site-specific foci dynamics and improve our hypothetical model.
Eventually, an interesting long term perspective could be to export our reporter systems in other *Brucella* strains displaying intriguing genomic particularities, such as *Brucella suis* biovar 3, where the two chromosomes are fused in one single 3.1 Mb chromosome (Jumas-Bilak *et al.* 1998), or *Brucella microti*, which displays highly reduced cell cycle duration (about 30 min), thus suggesting several chromosome replication initiation events could occur per cell cycle (Jiménez de Bagüés *et al.* 2011).

Material & methods

Material and methods

Bacterial strains, growth conditions, plasmids and cell lines.

Escherichia coli host strain DH10B or S17-1 was cultivated on Solid Luria-Bertani (LB) or liquid LB medium at 37°C. Brucella abortus 544 strains were cultivated on solid or liquid 2YT medium at 37°C. Antibiotics were used at the following final concentrations: ampicilline 100 µg/ml; kanamycine 50 µg/ml (for E. coli) and 10 µg/ml (for B. abortus); chloramphenicol 20 µg/ml; nalidixic acid 25 µg/ml. Plasmids used in this study were pGEM5-Zf(+) (Promega®, Madison, USA), pKS-*ori*T cat, pBBR1, pMR10-*kan*, and pNPTS138.

Polymerase Chain Reaction.

-**Diagnostic PCR:** The PCR mix was composed of dNTPs (5 mM each), primers (20 □M each), GoTaq polymerase (Promega®, Madison, USA), 5X GoTaq buffer (1X) and template DNA (about 70 ng). After a first denaturation step at 94°C for 4 min, program was made of 30 amplification cycles composed of a first denaturation step (30 s at 94°C), a hybridization step (30 s at a suitable temperature regarding primers predicted Tm) and a final elongation step at 72°C (1 min/kb, duration depending on the expected amplification product size). A final elongation step was made for 10 min at 72°C. Size-approximation and absence of aspecific amplification products were checked by electrophoresis migration on a 1% agarose gel (2% agarose if amplified fragment size below 250bp) supplemented with ethidium bromide to visualize DNA using UV light. The fragment size marker used was the GeneRulerTM 1kb DNA Ladder (Fermentas).

-**Preparative PCR:** The PCR mix was composed of dNTPs (5 mM each), primers (20 □M each), Phusion polymerase (0.02 U/□l, Finnzymes), 5X Phusion buffer (1X) and template DNA (about 70 ng). After a first denaturation step at 98°C for 30 s, program was made of 30 amplification cycles composed of a first denaturation step (10 s at 98°C), a hybridization step (30 s at a suitable temperature regarding primers predicted Tm) and a final elongation step at 72°C (30 s/kb, duration depending on the expected amplification product size). A final elongation step was made for 10 min at 72°C. Size-approximation and absence of aspecific amplification products were checked by electrophoresis migration.

PCR products purification

The PCR products purification on column was made using the MSB SpinPCRapace (Invitek, Berlin, Germany) and following the manufacturer's protocol.

Ligation protocol.

Ligation mix was composed of 5X ligase buffer (1X), restricted vectors and inserts sequences (volumes used based on respective concentrations in order to obtain a 1/10 ratio), 5X ligase buffer (1X), and T4-ligase (Fermentas). The final mix was incubated overnight at 18°C.

Transformation with CaCl2-competent DH10B E. coli.

50 µl of competent bacterial cells were put on ice and 5 µl of DNA were added. The mix was then incubated for 20 min on ice before a 2 min thermic shock at 42°C. Cells were then resuspended with 700 µl liquid LB and place at 37°C for 45 min. The culture was finally centrifuged 3 min at 5000 rpm and the obtained pellet was resuspended in 100 µl of supernatant before being spread onto solid LB containing the appropriate antibiotic for an overnight culture.

Plasmid extraction.

E. coli was cultivated overnight in liquid LB at 37°C, then, centrifugated 1 min at 13000 rpm. The pellet was resuspended in 300 µl of P1 solution (RNAase A 100 µg/ml, Tris HCl 50 mM, EDTA 80 mM, pH 8, 4°C), followed by 300µl of P2 lysis solution (NaOH 100 mM, SDS 1%). After 5 min, P2 was neutralized by the P3 solution (KAc 3 M, pH 5.5) and the lysate was centrifuged for 10 min at 13000 rpm. The supernatant was transferred to a new tube and 700 µl of isopropanol was added. The mix was then centrifugated for 10 min at 13000 rpm. Supernatant was discarded and pellet was washed in 400 µl of cold 70% ethanol. After a 5 min centrifugation at 13000 rpm, the supernatant was discarded and the pellet was dried then resuspended in ddH2O (milliQ purification system, Millipore).

Enzymatic restriction.

DNA was incubated with the appropriate restriction enzyme(s) (10 U/µl) (Roche®), 10X appropriate buffer (1X), incubated for 1h to 1h30 depending on the amount of DNA to be restricted.

Mating.

First, 50 µl of a culture of conjugative E. coli S17-1 strain carrying the plasmid of interest were mixed with 1ml of culture of B. abortus strain. The culture was then centrifugated for 2 min at 7000 rpm. The supernatant was discarded and the pellet was resuspended in 1 ml of liquid 2YT medium. This suspension was then centrifugated again for 2 min at 7000 rpm and the obtained pellet was resuspended in a small fraction of the supernatant before being spread as a single drop onto solid 2YT and placed at 37°C overnight.

For integrative plasmids (e.g. pNPTS138), half of the drop was harvested and spread on solid 2YT supplemented with kanamycine and nalidixic acid and placed at 37°C for 3 to 5 days. Then, the obtained colonies were streaked on solid 2YT supplemented with kanamycine but no nalidixic acid. Afterward, one of the streak was incubated in liquid 2YT with no antibiotic for 36h in order to allow bacteria to lose the integrated plasmid. 100 ml of this culture was

then spread onto solid 2YT supplemented with sucrose (5%). Clones growing on this medium were finally spread on both solid 2YT supplemented with kanamycine and on solid 2YT supplemented with sucrose, and clones growing only 2YT supplemented with sucrose were selected for further PCR screenings.

Fill-in

At 4°C, mix restricted and purified DNA fragment (0.5 to 2.5 µg) with 1 µl of T4 DNA polymerase (5 U/µl) (Invitrogen), 1 µl of 5 mM dNTP mix, and 10 µl of T4 DNA polymerase buffer. Add water to reach a total volume of 50 µl. Incubate at 11°C for 15 minutes. Place on ice. Inactivate T4 DNA polymerase by phenol chloroform extraction or column purification (see "PCR products purification") coupled to heat inactivation (80°C for 20 minutes).

TRSE labeling

Centrifuge 1 ml of cells for 2 minutes at 7500 rpm. Remove supernatant and resuspend the pellet in 1ml of PBS. Repeat these two steps once again to correctly wash the cells in order to remove as much medium-borne amine groups as possible as they could interfere with proper TRSE staining. In the meantime, dilute Texas Red®-X, Succinimidyl Ester (Invitrogen) in PBS at a concentration of 1 µg/ml. Centrifuge cells for 2 minutes at 7500 rpm and resuspend using fresh PBS-diluted TRSE solution. Incubate in the dark for 15 minutes at room temperature. Afterward, pellet cells by centrifuging for 2 minutes at 7500 rpm, resuspend in PBS in order to wash TRSE excess. Then, centrifuge (the pellet should display a reddish/purplish color) and resuspend in 1 ml of 2YT. Check proper staining under the microscope using the mCherry fluorescence channel (cells must be entirely labeled) (optional). If proper staining, incubate cells for 45 minutes at 37°C under agitation. This step allows the cells to grow and thus to synthesize and incorporate unlabeled material, therefore highlighting the growing zone by counter-staining. After this incubation time, observe cells under the microscope.

Microscopy

The microscope which has been used is a Nikon Eclipse E1000 (objective 100X, plan Apo) connected to a Hamamatsu ORCA-ER camera. We also used DF type immersion oil (Nikon oil) with refraction a indice of 1.5150 +/- 0.0002.

Agarose pad construction

A 1% agarose PBS solution is heated until dissolution of agarose and stored at 55°C for several days/weeks. Pour 350 µl of the hot agarose solution between two slightly spaced parallel microscopy slides and wait until the agarose solution solidifies. Then, remove the top microscopy slide in order to conserve the pad on a single slide. To prevent pads from drying, transiently store them in a petri dish containing a piece of water-soaked paper towel.

Coverslip mounting

Place 2 µl drop of the culture you wish to observe on the center of an agarose pad and place a coverslip on the top of the drop. Once the drop has spread, cut off the excess of agarose in order to conserve a single square delimited by the surface of the coverslip. When performing this step, take care not to press on the coverslip as it will deform the pad (which needs to remain flat in order to obtain decent images). Then, seal the pad by spreading hot VALAP (mix of equal amounts of paraffin, lanoline and vaseline) on the edges of the coverslip. When cooling down, the valap will solidify and form a solid crust preventing the bacteria from accessing the outside. Slides are now ready to be observed.

FACS analyses

Bacteria fixation

First, inoculate a fresh colony of your strain into 5 ml 2YT medium and grow overnight at 37° C. Then, dilute the overnight culture until the culture reaches an exponential growth phase (typically between O.D. 600nm 0.4 to 0.6). Transfer 1 ml of this culture into 9 ml of an ice cold 77 % ethanol solution in a 15 ml tube and mix well. Finally, samples are stored at -20° C (up to 2 months). *Brucella* is killed at least after one hour in the solution.

Bacteria staining

First, centrifuge 2 ml of the fixed cells for 2' at 8000 rpm, discard the supernatant and resuspend the pellet in 2 ml FACS Staining Buffer. Harvest cells by centrifugation at 8000 RPM for 2' and resuspend the pellet in 1 ml of FACS Staining Buffer in which 5 µl of 20 mg/ml RNAseA (0.1 mg/ml) has been added and incubate at RT for 30'. Then, harvest cells by centrifugation at 8000 rpm for 2 minutes and remove supernatant. Resuspend the pellet in 1 ml FACS Staining Buffer in which 0.1 µl of 5 mM Sytox Green (Invitrogen) (0.5 µM) has been added and incubate at RT in the **dark** for 15 min. Eventually, analyze in flow cytometer (FACS SCAN, Argon Laser excitation at 488nm). The optimal cell number for flow cytometer: ~10^7/ml. If necessary dilute the cells 1:10 in staining buffer containing 0.5 µM Sytox Green.

FACS Staining Buffer (pH 7.2)

1 M Tris	5 ml (10 mM)
0.5 M EDTA	1 ml (1 Mm)
1 M NaCitrate	25 ml (50 mM)
TritonX-100	50 µl (0.01 %)
dH_2O to	**0.5 L**

Filtrate in order to sterilize and remove dust particles.

FACS parameters

Detector	Voltage	AmpGain	MODE	Gate
FSC	E01	1.00	LOG	No
SSC	631	1.00	LOG	No
FL1 (Alexa 488)	613	1.00	Lin	200 and above

(FSC: Forward Scatter, SSC: Side Scatter, FL1: fluorescence channel 1)

Gating

First, the wild-type strain is analyzed alone. Based on the obtained profile, the FACS detection parameters are standardized (or gated) in order to set a lower limit of fluorescence intensity detection. Such gating allows ignoring numerous hits displaying low level fluorescence intensity (i.e. Sytox Green-unlabeled cells or dust particles) which could bias the overall counts monitoring and associated analyses. Typical FL1 gate value delimitate an interval set at 200 units and above, with no maximal limit.

Annexes

Figure 24

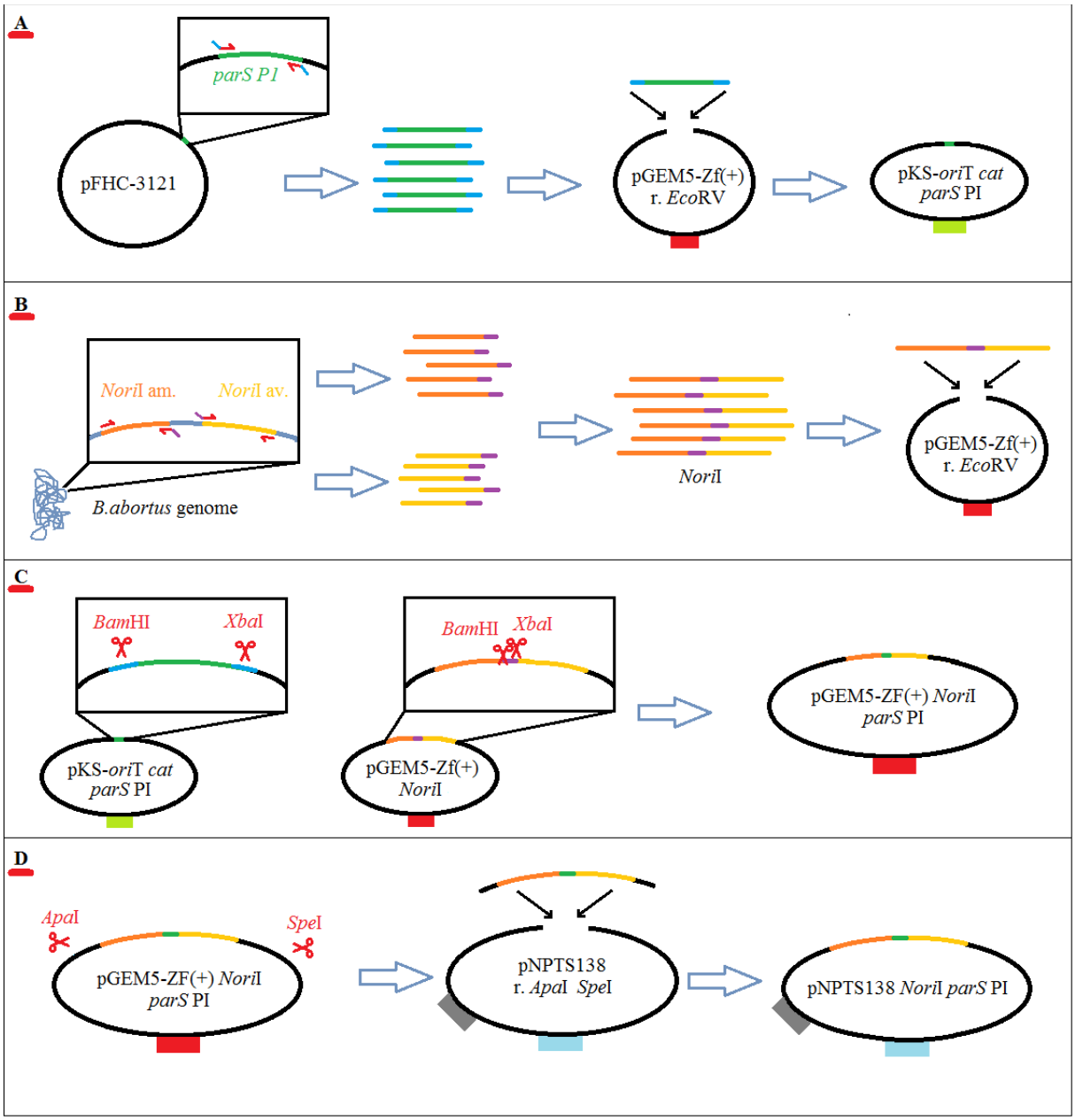

Insertion of *parS** into plasmids carrying chromosomal region of interest. A) PCR amplification of *parS* P1, ligation in a *Eco*RV restricted pGEM5-Zf(+) carrying an ampicilline resistance cassette (red rectangle), followed by transformation, clonal amplification, plasmidic extraction, enzymatic restriction using *Bam*HI and *Xba*I and ligation of the obtained fragment in a *Bam*HI and *Xba*I restricted pKS-oriT cat vector carrying a chloramphenicol resistance cassette (green rectangle). B) Separate PCR amplification of both upstream and downstream fragments of *Nori*I, linking PCR, and cloning of the reformed *Nori*I region + linker in pGEM5-ZF(+), followed by transformation, clonal amplification and plasmidic extraction. C) restriction of both pGEM5-ZF(+) *Nori*I and pKS oriT cat *parS* P1 using *Bam*HI and *Xba*I and ligation, forming pGEM5-ZF(+) *Nori*I *parS* P1, followed by transformation, clonal amplification and plasmidic extraction. D) restriction of both pGEM5-ZF(+) *Nori*I *parS* P1 and pNPTS138, carrying of kanamycine resistance cassette (blue rectangle) and a sucrose sensitivity cassette (grey rectangle), using *Apa*I and *Spe*I, and ligation, forming the final pNPTS138 *Nori*I *parS* P1.

Annex 1: Strains construction

Insertion of *parS** into plasmids carrying chromosomal regions of interest

In this section, the insertion of *parS* P1 inside a plasmid carrying *B. abortus Nori*I region will be detailed and used as a general example, considering the fact that all other insertion events (insertion of either *parS* P1 or *parS* pMT1 in *B. abortus Nori*I, *Nori*II, *Nter*I, *Nter*II, and *NdnaA* region-carrying plasmid) follow the same procedure. Plasmids generated by this method will be used to perform allelic replacement at targeted chromosomal loci, resulting in a "clean" insertion of *parS** in *B. abortus* without other sequences such as plasmids or antibiotic resistance cassette (see "Allelic replacement").

First, *parS* P1 was amplified by PCR from the pFHC-3212 plasmid (Nielsen *et al.* 2006), using primer P-*parS*-P1-F and P-*parS*-P1-R (see primer table for primers sequences). The resulting PCR product was then checked ligated in an EcoRV-restricted pGEM5-Zf(+) plasmid, using blunt-ends compatibility (see figure 24.A). After *E. coli* DH10B strain transformation, plasmidic extraction was performed on each culture and the obtained material was tested by diagnostic restriction. Plasmids displaying the expected migration profile were then sequenced and those with the correct sequence were restricted using *Bam*HI and *Xba*I (restriction sites initially present in the 5' tail of P-*parS*-P1-F/R primer respectively) in order to obtain an excised *parS* P1 sequence flanked with incompatible "sticky" ends. In the same way, a pKS-oriT cat plasmid (carrying a chloramphenicol resistance cassette) was restricted using the same enzymes. Next, a ligation was performed with these *Bam*HI-*Xba*I fragments, resulting in the oriented cloning of *parS* P1 in pKS-oriT cat, forming the pKS-oriT cat *parS* P1 plasmid (see figure 24.A).

In the meantime, two fragments of a specific chromosomal region (in this case, upstream *Nori*I and downstream *Nori*I, of both 750bp) were separately amplified by PCR from *B. abortus* genome (see primer table for primers sequences). Then, a thrid PCR or "linking-PCR" was performed based on specific primer-borne linker sequence complementarity, using primer P-*Nori*I-upstream-F and P-*Nori*I-downstream-R, resulting in a linkage of the upstream and downstream regions of *B. abortus Nori*I. Afterward, the newly reformed *Nori*I region (now carrying a linker sequence containing both a *Bam*HI and a *Xba*I restriction site) was ligated in an EcoRV restricted pGEM5-Zf(+) plasmid, forming pGEM5-Zf(+) *Nori*I (see figure 24.B) which was then transformed in CaCl2-competent *E. coli* DH10B strain.

Next, both pGEM5-Zf(+) *Nori*I and pKS-oriT cat *parS* P1 were separately restricted using *Bam*HI and *Xba*I, resulting in the excision of a *parS* P1 sequence flanked with incompatible "sticky" ends from the pKS-oriT cat *parS* P1 plasmid and in the digestion of the pGEM5-Zf(+) *Nori*I plasmid in its linker-borne *Bam*HI and *Xba*I restriction sites. Then, the two resulting restriction mixes were combined in a ligation in order to obtain pGEM5-Zf(+) *Nori*I *parS* P1 (see figure 24.C) and this mix was transformed in CaCl2-competent *E. coli* DH10B strain.

Figure 25

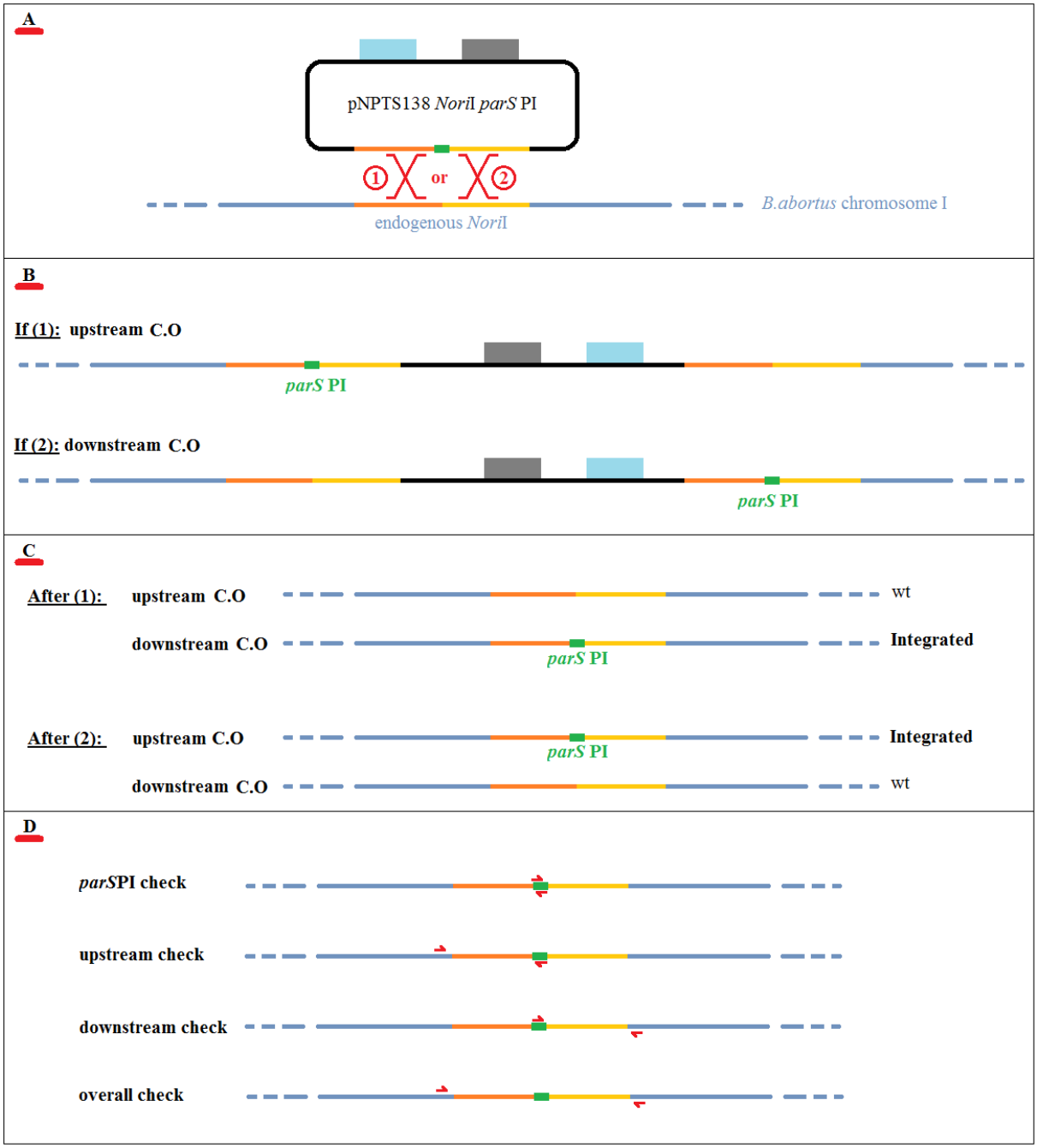

Allelic replacement in *B. abortus* using pNPTS138 *Nori*I *parS* P1. A) Schematic representation of the two possible theoretical crossing-over events between pNPTS138 *Nori*I *parS* P1 and *B. abortus* chromosome I. B) Possible results for plasmid integration, based on the location of the first crossing-over (either in the upstream or downstream region of *Nori*I). C) Possible results for plasmid excision, depending on the location of both first and second crossing-over events. D) Schematic illustration of the four PCRs performed in order to check for the correct insertion of *parS* P1 at the targeted locus.

Then, clones were randomly selected and tested for *parS* P1 integration in *Nori*I by diagnostic PCR, using primer P-*Nori*I-upstream-F and P-*parS*-P1-R (see primer table for primer sequences). A plasmidic extraction was then performed on each positive colony after overnight culture and the obtained material was checked by diagnostic restriction. Then, plasmids displaying the correct digestion pattern were restricted using *Apa*I and *Spe*I sites flanking the *Nori*I region of the pGEM5-Zf(+) *Nori*I *parS* P1 plasmid. In the meantime, a pNPTS138 plasmid (carrying both a kanamycine resistance cassette and *sacB*, a sucrose sensitivity cassette) was restricted using the same enzymes. These two restriction mixes were then combined in ligation in order to obtain pNPTS138 *Nori*I *parS* P1 (see figure 24.D), and the resulting mix was transformed in $CaCl_2$-competent *E. coli* DH10B strain. Eventually, after plasmidic extraction and diagnostic restriction, the pNPTS138 *Nori*I *parS* P1 plasmid was finally transformed in conjugative $CaCl_2$-competent *E. coli* S17-1 strain.

Allelic replacement

Once obtained and checked, one clone of *E. coli* S17-1 pNPTS138 *Nori*I *parS* P1 and a sample of *B. abortus* 544 wt are separately cultured overnight. The next day, mating is engaged as described in the material and methods section. Once again, only the allelic replacement of pNPTS138 *Nori*I *parS* P1 in *B. abortus* chromosome I will be detailed, since all others allelic replacement events follow the same procedures.

Once inside *B. abortus*, the pNPTS138 *Nori*I *parS* P1 plasmid can be integrated by a specific crossing-over event (C.O.) in *B. abortus* chromosome I. This event, happening thanks to sequence identity between the chromosome-borne *Nori*I and the plasmid-borne *Nori*I *parS* P1 (750bp both upstream and downstream of *parS* P1), can either occur in the upstream or downstream region of *Nori*I (see figure 25.A), resulting in two different integration configurations (see figure 25.B). Consequently to the first C.O. event, the pNPTS138 *Nori*I *parS* P1 plasmid is fully integrated inside *B. abortus* chromosome I, presumably at the targeted locus, therefore conferring kanamycine resistance as well as sucrose sensitivity to the bacterium. Then, one colony able to grow on plates supplemented with kanamycine is randomly selected and cultured in liquid phase (without kanamycine) for a 36h growth period, therefore relieving the selective pressure initially induced by the antibiotic. This step allows the C.O.-mediated excision of the integrated plasmid while keeping *parS* P1 integrated at the targeted locus (with a theoretical frequency of 50%). A fraction of this culture is then spread on a plate supplemented with sucrose in order to select bacteria which have excised the integrated plasmid (and therefore, lost the plasmid-borne sucrose sensitivity cassette). However, after this plasmid excision step, two final configurations were possible, depending on the location of the two C.O. involved in integration and excision. In fact, if both the first and the second C.O. happened in the same region (either upstream or downstream), the entire plasmid (including its *parS* P1 sequence) would have been excised, resulting in a return to the wild type situation (see figure 25.C). Conversely, if the two C.O. happened in different fragments of the *Nori*I region (either “upstream-downstream” or “downstream-upstream”),

this would result in the expected allelic replacement, i.e. integration of *parS* P1 at the targeted locus (see figure 25.C).

To screen for allelic replacement events, we have first randomly selected colonies able to grow on solid 2YT (*Brucella* standard culture medium) supplemented with sucrose and streaked them on two different types of media: first, on a solid 2YT kanamycine plates, followed by solid 2YT sucrose plates. In this way, clones able to grow on 2YT sucrose but not on 2YT kanamycine suggest excision of the previously integrated pNPTS plasmid (characterized by the loss of both kanamycine resistance and sucrose sensitivity). Moreover, if mutations are generated in *sacB* (the frequently mutated sucrose sensitivity cassette encoded in pNPTS138), integrants could display a sucrose-resistant phenotype with no excision of the plasmid. However, thanks to our two-step screening, these mutated clones also display a plasmid-borne kanamycine resistance and can thus be eliminated from further investigations.

Next, clones simultaneously displaying a sucrose-resistant and kanamycine-sensitive phenotype were selected and four diagnostic PCRs were performed. First, the presence of *parS* P1 itself in the colonies was checked using primers P-*parS*-P1-F and P-*parS*-P1-R. Then, clones positive for this first PCR were selected for two other PCRs (see figure 25.D). The second PCR was designed to check the insertion of *parS* P1 at the expected locus, using a chromosomal region located upstream of the *Nori*I recombination site. To do so, we combined a new chromosome hybridizing primer, P-check-*Nori*I-upstream-F (see primer table for primers sequences), hybridizing upstream of the *Nori*I recombination site, with P-*parS*-P1-R. The third PCR was also designed to check the insertion of *parS* P1 at the expected locus, but using the downstream region of *Nori*I. We thus combined P-*parS*-P1-F with a second chromosome hybridizing primer, P-check-*Nori*I-downstream-R (see primer table for primers sequences), hybridizing downstream of the *Nori*I recombination site (see figure 25.D).

Finally, a fourth PCR was performed in order to check the integration of only one single *parS* P1 sequence at the *Nori*I locus. To do so, the entire *Nori*I recombination site is amplified using primers P-check-*Nori*I-downstream-F and P-check-*Nori*I-downstream-R. The resulting PCR product then undergoes diagnostic restriction using *Bam*H1 (which restriction site is only present in the inserted *parS** sequence and not in the endogenous *Nori*I recombination site).

It should be noted that the integration of a second *parS** sequence in previously *parS*-integrated *B. abortus* strains (in order to generated strains with two *parS*-integrated chromosomal regions such as *B. abortus* 544 *Nori*I *parS* P1 *Nori*II *parS* pMT1), follows the same procedures as for a single *parS* insertion. The only difference resides in the nature of the *Brucella* strain which is initially selected to undergo mating.

Construction of the *xfp-parB** fusion carrying plasmids

In order to localize the *parS** sequence inserted in a specific chromosomal region of interest, the *parS**-binding protein ParB* (either ParB P1 or ParB pMT1, depending on the *parS* sequence used) was fused to a *parS**/ParB* specific fluorescent protein (XFP). The two fusion proteins used in this work are **CFPEc-ParB P1** and **yGFP-ParB pMT1** (displaying CFP-like and YFP-like emission spectrums respectively).

First, both fusion genes were amplified by PCR from two plasmids: pFHC2896 (Nielsen *et al.* 2006), using primers P-cfpEc-parB P1-F and P-cfpEc-parB P1-R for cfpEc-parB P1 amplification, and pMS319 (Toro *et al.* 2008), using primers P-ygfp-parB pMT1-F and P-ygfp-parB pMT1-R for ygfp-parB pMT1 amplification (see primer table for primers sequences). The two fragments were initially separately ligated in *Eco*RV restricted pGEM5-Zf(+), and the resulting ligation mix was engaged in transformation of CaCl2-competent *E. coli* DH10B strains.

However, due to unspecified reasons (possibly toxicity issues of the expected construct), diagnostic restriction patterns of several plasmidic extractions of theoretical pGEM5-Zf(+) cfpEc-parB P1 never displayed the expected profile. Consequently, the pGEM5-Zf(+) vector was replaced by a lower copy number pBBR1 plasmid for cfpEc-parB P1 subcloning. It should be noted that this issue only involved the cfpEc-parB P1 fusion, such problems were not encountered with the ygfp-parB pMT1 fusion.

After sequencing and plasmidic extractions, each plasmid was specifically restricted in order to obtain an excised fusion gene with incompatible "sticky" ends (using *Hind*III and *Xba*I for the ygfp-parB pMT1 fusion, and using *Xba*I and *Bam*H1 for the cfpEc-parB P1 fusion). In the meantime, pMR10-*kan* (a low copy plasmid known for being stable in *Brucella spp.*) was restricted in two separate mixes using the same couples of enzymes. Finally, two separate ligation were performed in order to obtain **pMR10-*kan* ygfp-parB pMT1** and **pMR10-*kan* cfpEc-parB P1**, and the two resulting mixes were transformed in CaCl2-competent *E. coli* DH10B strain.

Meanwhile, a third plasmid in which both fusions genes were placed in one single pMR10-*kan* vector was constructed. To do so, a single step triple ligation involving both fusions excised from their respective vectors and a *Hind*III *Bam*H1 restricted pMR10-*kan* was performed in order to obtain **pMR10-*kan ygfp-parB* pMT1 *cfpEc-parB* P1**. This third plasmid enables us to follow both *parS** sequences at the same time in a strain possessing both *parS** sequences by expressing both fusion genes from a single vector, thus getting rid of the plasmid incompatibility issue inherent to the simultaneous use of two pMR10-*kan* vectors.

Once again, due to unspecified reasons, diagnostic restriction patterns of several plasmidic extractions of theoretical pMR10-*kan cfpEc-parB* P1 never displayed the expected profile. In this case however, toxicity did not appear to be the most plausible cause since strains carrying the pMR10-*kan ygfp-parB* pMT1 *cfpEc-parB* P1 plasmid grew normally while expressing both fusions.

To tackle this technical problem, we decided to use the pMR10-*kan ygfp-parB* pMT1 cfpEc-parB-P1 plasmid (carrying both fusion genes) and to excise the *ygfp-parB* pMT1 fusion in order to only conserve the *cfpEc-parB* P1 fusion. To do so, *ygfp-parB pMT1* was excised using *Hind*III and *Xba*I. Then, incompatible "sticky ends" of the resulting DNA fragments were "filled" in order to create blunt ends according to the "fill-in" protocol (see "Material and methods"). The resulting mix was then engaged in ligation in order to self-ligate the linearized plasmid of interest.

Additionally, each of the three inserts (*ygfp-parB* pMT1, *cfpEc-parB* P1, and *ygfp-parB* pMT1 *cfpEc-parB* P1) were placed in a pBBR vector (common overexpression vector widely used in *Brucella spp.*). The goal of this manipulation was to tackle in advance a possibly insufficient expression level of the fusion proteins due to the extremely low copy number of the pMR10-*kan* vector. Fortunately, this problem was not encountered.

Annex 2: Strain and primers tables

Strain tables

***E. coli* DH10B**	pGEM5-Zf(+) *parS* P1
	pGEM5-Zf(+) *parS* pMT1
	pKS-*ori*T *cat parS* P1
	pKS-*ori*T *cat parS* pMT1
	pGEM5-Zf(+) *Nori*I
	pGEM5-Zf(+) *Nter*I
	pGEM5-Zf(+) *Nori*II
	pGEM5-Zf(+) *Nter*II
	pGEM5-Zf(+) *NdnaA*
	pGEM5-Zf(+) *Nori*I *parS* P1
	pGEM5-Zf(+) *Nori*I *parS* pMT1
	pGEM5-Zf(+) *Nter*I *parS* P1
	pGEM5-Zf(+) *Nter*I *parS* pMT1
	pGEM5-Zf(+) *Nori*II *parS* P1
	pGEM5-Zf(+) *Nori*II *parS* pMT1
	pGEM5-Zf(+) *Nter*II *parS* P1
	pGEM5-Zf(+) *Nter*II *parS* pMT1
	pGEM5-Zf(+) *NdnaA parS* pMT1
	pNPTS138 *Nori*I *parS* P1
	pNPTS138 *Nori*I *parS* pMT1
	pNPTS138 *Nter*I *parS* P1
	pNPTS138 *Nter*I *parS* pMT1
	pNPTS138 *Nori*II *parS* P1
	pNPTS138 *Nori*II *parS* pMT1
	pNPTS138 *Nter*II *parS* P1
	pNPTS138 *Nter*II *parS* pMT1
	pNPTS138 *NdnaA parS* pMT1
	pGEM5-Zf(+) *cfpEc-parB* P1
	pGEM5-Zf(+) *ygfp-parB* pMT1
	pGEM5-Zf(+) *ygfp-parB* pMT1 *cfpEc-parB* P1
	pMR10-*kan cfpEc-parB* P1
	pMR10-kan *ygfp-parB* pMT1
	pMR10-kan ygfp-parB pMT1 cfpEc-parB P1

***E. coli* S17-1**	pNPTS138 *Nori*I *parS* P1
	pNPTS138 *Nori*I *parS* pMT1
	pNPTS138 *Nter*I *parS* P1
	pNPTS138 *Nori*II *parS* P1
	pNPTS138 *Nori*II *parS* pMT1
	pNPTS138 *Nter*II *parS* P1
	pNPTS138 *Nter*II *parS* pMT1
	pNPTS138 *NdnaA parS* pMT1
	pMR10-*kan cfpEc-parB* P1
	pMR10-kan *ygfp-parB* pMT1
	pMR10-kan ygfp-parB pMT1 cfpEc-parB P1

***B. abortus* 544**	pMR10-kan *cfpEc-parB* P1
	pMR10-kan *ygfp-parB* pMT1
	pMR10-kan *ygfp-parB* pMT1 *cfpEc-parB* P1
	*Nori*I *parS* P1
	*Nori*I *parS* pMT1
	*Nter*I *parS* P1
	*Nori*II *parS* pMT1
	*Nter*II *parS* pMT1
	*Nori*I *parS* P1 pMR10-kan ygfp-parB pMT1 cfpEc-parB P1
	*Nori*I *parS* pMT1 pMR10-kan ygfp-parB pMT1 cfpEc-parB P1
	*Nter*I *parS* P1 pMR10-kan ygfp-parB pMT1 cfpEc-parB P1
	*Nori*II *parS* pMT1 pMR10-kan ygfp-parB pMT1 cfpEc-parB P1
	*Nter*II *parS* pMT1 pMR10-kan ygfp-parB pMT1 cfpEc-parB P1
	*Nori*I *parS* pMT1 N*ter*I *parS* P1
	*Nori*II *parS* pMT1 *Nter*II *parS* P1
	*Nori*I *parS* P1 *Nori*II *parS* pMT1
	*Nter*I *parS* P1 *Nter*II *parS* pMT1
	*Nori*I *parS* P1 *NdnaA parS* pMT1
	*Nori*I *parS* pMT1 N*ter*I *parS* P1 pMR10-kan ygfp-parB pMT1 cfpEc-parB P1
	*Nori*II *parS* pMT1 *Nter*II *parS* P1 pMR10-kan ygfp-parB pMT1 cfpEc-parB P1
	*Nori*I *parS* P1 *Nori*II *parS* pMT1 pMR10-kan ygfp-parB pMT1 cfpEc-parB P1
	*Nter*I *parS* P1 *Nter*II *parS* pMT1 pMR10-kan ygfp-parB pMT1 cfpEc-parB P1
	*Nori*I *parS* P1 *NdnaA parS* pMT1 pMR10-kan ygfp-parB pMT1 cfpEc-parB P1

Primers table

parS P1	P-parS-PI-F	gctctagaaaactttcgccattcaaattt
	P-parS-PI-R	cgggatccccaaggtgaaatcgtggc
parS pMT1	P-parS-pMTI-F	gctctagatgtttttcaccacgccaa
	P-parS-pMTI-R	cgggatccgaggttgaaaagcgtggtg
NorI upstream	P-NorI-upstream-F	ttccgatctccacgccat
	P-NorI-upstream-R	tccggtggccgaccgtctagaaggctatgacgttcaaggaaaagg
NorI downstream	P-NorI-downstream-F	agacggtcggccaccggatccttgagcgcatcgcgaaa
	P-NorI-downstream-R	acattcagcgttgcggtca
NterI upstream	P-NterI-upstream-F	gcctttctacggcttaacaccag
	P-NterI-upstream-R	tccggtggccgaccgtctagagggacatgaggatgctgatg
NterI downstream	P-NterI-downstream-F	agacggtcggccaccggatccatgccaagatgaccgctagtg
	P-NterI-downstream-R	tggctgacatggggattg
NdnaA upstream	P-NdnaA-upstream-F	atccggcaaggctgaatg
	P-NdnaA-upstream-R	tccggtggccgaccgtctagatagggctttgcttttcaaggt
NdnaA downstream	P-NdnaA-downstream-F	agacggtcggccaccggatcccgccgataccattaacaatacg
	P-NdnaA-downstream-R	attcatgccgacgtcctatc
NorII upstream	P-NorII-upstream-F	cgcaaattctggcaggattat
	P-NorII-upstream-R	tccggtggccgaccgtctagaggctgtctttttaaggccg
NorII downstream	P-NorII-downstream-F	agacggtcggccaccggatccgcccgatccggtacttatattc
	P-NorII-downstream-R	gacaggtccgcgtctttc
NterII upstream	P-NterII-upstream-F	ttgagaaactcgatgccgg
	P-NterII-upstream-R	tccggtggccgaccgtctagatcaaaaatggcaaccgcc
NterII downstream	P-NterII-downstream-F	agacggtcggccaccggatccgagacatgttttaaccagccgg
	P-NterII-downstream-R	agattacaatcgacgtcgtttcg
ygfp-parB pMTI	P-ygfp-parB pMTI-F	cccaagcttatggtgagcaagggcga
	P-ygfp-parB pMTI-R	gctctagacgaccgttactcacctgattctggaagtctt
cfpEc -parB PI	P-cfpEc-parB PI-F	gctctagaatgataataaggaggccatatgtctaaagg
	P-cfpEc-parB PI-R	cgggatccttaaggcttcggctttttatc
B. ab chrm integ. Check	P-check-NorI-upstream-F	tgcaaccgcagcacagatcgc
	P-check-NterI-upstream-F	atttccgcaccgaaccaccgg
	P-check-NdnaA-upstream-F	gaggatgcgatccgcgcttcc
	P-check-NorII-upstream-F	aagtggccacccccttccatcc
	P-check-NterII-upstream-F	gatgcccgacgaagtgcagcat
	P-check-NorI-downstream-R	atggatgcgagaaggttgag
	P-check-NterI-downstream-R	tggatgctgtcgatatttcct
	P-check-NdnaA-downstream-R	atgaaaccgccatgaaaagct
	P-check-NorII-downstream-R	accggacggacgaaaagac
	P-check-NterII-downstream-R	catggagatgccgcaatgac

Annex 3 : References

Brown PJ, de Pedro MA, Kysela DT, Van der Henst C, Kim J, De Bolle X, Fuqua C, Brun YV. (2012 Jan) Polar growth in the Alphaproteobacterial order Rhizobiales. Proc Natl Acad Sci U S A. 109(5): 1697-701.

Celli J, Salcedo SP, Gorvel JP. (2005 Feb) Brucella coopts the small GTPase Sar1 for intracellular replication. Pro Natl Acad Sci USA. 102(5): 1673-8.

Cervantes-Rivera R, Pedraza-Lopez F, Pérez-Sequra G, Cevallos MA. (2011 Jan) The replication origin of a repABC plasmid. BMC Microbiol. 11: 158.

Cevallos MA, Cervantes-Rivera R, Gutiérrez-Rios RM. (2008 Jul) The *repABC* plasmid family. Plasmid. 60(1): 19-37.

Chain PS, Comerci DJ, Tolmasky ME, Larimer FW, Malfatti SA, Vergez LM, Aguero F, Land ML, Ugalde RA, Garcia E. (2005) Whole-genome analyses of speciation events in pathogenic brucellae. Infect. Imm. 73(12): 8353-61.

Collier J. (2012 Mar) Regulation of chromosomal replication in *Caulobacter crescentus*. Plasmid. 67(2):76-87.

Corbel, M. J., and W. J. Brinley-Morgan. 1984. Genus Brucella. *In*: N. R. Krieg and J. C. Holt (Eds.) Bergey's Manual of Systematic Bacteriology. Williams and Wilkins. Baltimore, MD. 1:377-388.

Duggin IG, Bell SD. (2009 Apr) Termination structures in the Escherichia coli chromosome replication fork trap. J Mol Biol. 378(3): 532-9.

Easter J Jr, Gober JW. (2002 Aug) ParB-stimulated nucleotide exchange regulates a switch in functionally distinct ParA activities. Mol Cell. 10(2): 427-34.

Fernandez C, Gonzalez D, Collier J. (2011 Oct) Regulation of the Activity of the Dual-Function DnaA protein in *Caulobacter crescentus*. PLoS One. 6(10): e26028.

Figge RM, Easter J, Gober JW. (2003 Mar) Productive interaction between the chromosome partitioning proteins, ParA and ParB, is required for the progression of the cell cycle in *Caulobacter crescentus*. Mol Microbiol. 47(5): 1225-37.

Frenchick PJ, Markham RJ, Cochrane AH. (1985 Feb) Inhibition of phagosome-lysosome fusion in macrophages by soluble extracts of virulent Brucella abortus. Am J Vet Res. 46(2): 322-5.

Haag AF, Arnold MF, Myka KK, Krescher B, Dall'angelo S, Zanda M, Mergaert P, Ferguson GP. (2012 Oct) Molecular insights into bacteroid development during Rhizobium-legume symbiosis. FEMS Microbiol Rev. Epub.

Hallez R, Bellefontaine AF, Letesson JJ, De Bolle X. (2004 Aug) Morphological and functional asymmetry in alpha-proteobacteria. Trends Microbiol. 12(8): 361-5.

Hallez R, Mignolet J, Van Mullem V, Wery M, Vandenhaute J, Letesson JJ, Jacobs-Wagner C, De Bolle X. (2007 Mar) The asymmetric distribution of the essential histidine kinase PdhS indicates a differentiation event in Brucella abortus. EMBO J. 26(5): 1444-55.

Halling SM, Peterson-Burch DB, Bricker BJ, Zuerner RL, Qing Z, Li LL, Kapur V, Alt DP, Oslen SC. (2005 Apr) Completion of the genome sequence of *Brucella abortus* and comparison to the highly similar genomes of *Brucella melitensis* and *Brucella suis*. J bacterial. 187(8): 2715-26.

Harry EJ. (2001 May) Bacterial cell division: regulation Z-ring formation. Mol Microbiol. 40(4): 795-803.

Jiménez de Bagüés MP, Ouahrani-Bettache S, Quintana JF, Mitjana O, Haana N, Bessoles S, Sanchez F, Scholz HC, Lafont V, Köhler S, Occhialinu A. (2012 Jul) The new species *Brucella microti* replicates in macrophages and causes death in murine models of infection.

Jumas-Bilak E, Michaux-Charachon S, Bourg G, O'callaghan D, Ramuz M. (1998 Jan) Differences in chromosome number and genome rearrangements in the genus *Brucella*. Mol Microbiol. 27(1): 99-106.

Jun S, Wright A. (2010 Aug) Entropy as the driver of chromosome segregation. Nat Rev Microbiol. 8(8):600-7.

Kahng LS, Shapiro L. (2003 Jun) Polar localization of replicon origins in the multipartite genomes of *Agrobacterium tumefaciens* and *Sinorhizobium meliloti*. J Bacteriol. 185(11): 3385-91.

Kaquni JM. (2011 Oct) Replication initiation at the *Escherichia coli* chromosomal origin. Curr Opin Chem Biol. 15(5): 606-613.

Lemon KP, Grossman AD. (2001 Aug) The extrusion-capture model for chromosome partitioning in bacteria. Genes Dev. 15(16):2031-41.

Li Y, Sergueev K, Austin S. (2002 Nov) The segregation of the Esherichia coli origin and terminus of replication. Mol Microbiol. 46(4):985-96.

Mackiewicz P, Zakrewska-Czerwinska J, Zawilak A, Dudek MR, Cebrat S. (2004 Jul) Where does the bacterial replication start? Rules for predicting the oriC region. Nucleic Acids Res. 32(13):3781-91.

Mierzejewska J, Jaqura-Burddzy G. (2012 Jan) Prokaryotic ParA-ParB-parS system link bacterial chromosome segregation with the cell cycle. Plasmid. 67(1): 1-14.

Mohl DA, Gober JW. (1997 Mar) Cell cycle-dependent polar localization of chromosome partitioning proteins in Caulobacter crescentus. Cell. 88(5): 675-84.

Moreno E, Moriyon I. (2006) The Genus *Brucella*. Prokaryotes. 5:315-456

Nielsen HJ, Ottesen JR, Youngren B, Austin SJ, Hansen GH. (2006 Oct) The *Escherichia coli* chromosome is organized with left and right chromosome arms in separate cell halves. Mol Microbiol. 62(2):331-8.

Paulsen IT, Seshadri R, Nelson KE, Eisen JA, Heidelberg JF, Read TD, Dodson RJ, Umayam L, Brinkac LM, Beanan MJ, Daugherty SC, Deboy RT, Durkin AS, Kolonay JF, Madupu R Nelson WC, Ayodeji B, Kraul M, Shetty J, Maled J, Van Aken SE, Riedmuller S, Tettelin H, Gill SR, White O, Salzberg SL, Hoover DL, Lindler LE, Halling SM, Boyle SM, Fraser CM. (2002 Oct). The *Brucella suis* genome reveals fundamental similarities between animal and plant pathogens and symbionts. Pro Natl Acad Sci USA. 99(20): 13148-13153.

Pinto UM, Pappas KM, Winans SC. (2012 Nov) The ABCs of plasmid replication and segregation. Nat Rev Microbiol. 10: 755-765.

Pitzschke A, Hirt H. (2010 Mar) New insights into an old story: Agrobacterium-induced tumour formation in plants by plant transformation. EMBO J. 29(6): 1021-32.

Rasmussen T, Jensen RB, Skovgaard O. (2007 Jul) The two chromosomes of *Vibrio cholera* are initiated at different time point in the cell cycle. EMBO J. 26(13): 3124-31.

Rodionov O, Lobocka M, Yarmolinsky M. (1999 Jan) Silencing of genes flanking the P1 plasmid centromere. Science. 283(5401):546-9.

Schofiel WB, Lim HC, Jacobs-Wagner C. (2010 Sep) Cell cycle coordination and regulation of bacterial chromosome segregation dynamics by polarly localized proteins. EMBO J. 29(18): 3068-81.

Shebelut CW, Guberman JM, van Teeffelen S, Yakhnina AA, Gitai Z. (2010 Jul) *Caulobacter* chromosome segregation is an ordered multistep process. Proc Natl Sci U S A. 107(32): 14194-14198.

Skerker JM, Laub MT. (2004 Apr) Cell-cycle progression and the generation of asymmetry in Caulobacter cresentus. Nat Rev Microbiol. 2(4): 325-37.

Sliusarenko O, Heinritz J, Emonet T, Jacobs-Wagner C. (2011 May) High-throughput, subpixel precision analysis of bacterial morphogenesis and intracellular spatio-temporal dynamics. Mol Microbiol. 80(3): 612-27.

Smith EF, Townsend CO. (1907) A Plant-Tumor of Bacterial Origin. Science. 25(643): 671-673.

Starr T, Ng TW, Wehrly TD, Knodler LA, Celli J. (2008 May) Brucella intracellular replication requires trafficking through the late endosomal/lysosomal compartment. Traffic. 9(5): 678-94.

Tomoyuki TU. (2010 Dec) Kinetochore-microtubule interactions: steps towards bi-orientation. EMBO J. 29(24): 4070-4082.

Toro E, Hong SH, Mc Adams HH, Shapiro L. (2008 Oct) *Caulobacter* requires a dedicated mechanism to initiate chromosome segregation. Pro Natl Acad Sci U S A. 105(40): 15435-40.

Toro E, Shapiro L. (2010 Feb) Bacterial Chromosome Organization and Segregation. Cold Spring Harb Perspect Biol. 2(2).

Tsokos CG, Laub MT. (2012 Nov) Polarity and cell fate asymmetry in Caulobacter crescentus. Curr Opin Microbiol. Epub S1369-5274(12)00151-8.

Van der Henst C, Beaufay F, Mignolet J, Didembourg C, Colinet J, Hallet B, Letesson JJ, De Bolle X. (2012 Oct) The histidine kinase PdhS controls cell cycle progression of the pathogenic alphaproteobacterium *Brucella abortus*. J Bacteriol. 194(19): 5305-14.

Viollier PH, Thanbichler M, McGrath PT, West L, Meewan M, McAdams HH, Shapiro L. (2004 Jun) Rapid and sequential movement of individual chromosomal loci to specific subcellular locations during DNA replication. Proc Natl Acad Sci U S A. 101(25): 9257-62.

Von Bargen K, Gorvel JP, Salcedo SP. (2012 May) Internal affairs: investigating the Brucella intracellular lifestyle. FEMS Microbiol Rev. 36(3):533-62.

Zakrewska J, Jakimowicz D, Zawilak-Pawlik A, Messer W. (2007 Jul) Regulation of the initiation of chromosomal replication in bacteria. FEMS Microbial Rev. 31(4): 378-87.